
Temporal Robustness in Discrete Time Linear Dynamical Systems

Nilava Metya
 Rutgers University
 New Brunswick, NJ
 nilava.metya@rutgers.edu

Arunesh Sinha
 Rutgers University
 New Brunswick, NJ
 arunesh.sinha@rutgers.edu

Abstract

Discrete time linear dynamical systems, including Markov chains, have found many applications. However, in some problems there is uncertainty about the time horizon for which the system runs. This creates uncertainty about the cost (or reward) incurred based on the state distribution when the system stops. Given past data samples of how long a system ran, we propose to theoretically analyze a distributional robust cost estimation task in a Wasserstein ambiguity set, instead of learning a probability distribution from a few samples. Towards this, we show an equivalence between a discrete time Markov Chain on a probability simplex and a global asymptotic stable (GAS) discrete time linear dynamical system, allowing us to base our study on a GAS system only. Then, we provide various polynomial time algorithms and hardness results for different cases in our theoretical study, including a fundamental result about Wasserstein distance based polytope.

1 Introduction

Discrete time linear dynamical systems, prominently Markov chains, have found many uses in machine learning [15] as well as other sciences [18], with applications in social networks [40], health [39, 31], and various other domains. There is a huge body of work on understanding the properties of such models [17], including asymptotic behavior and convergence rate analysis. In this work, we are motivated by works in health economics that utilize Markov Chain models to estimate the impact of disease spread within a given time frame, and not in the limit [11, 39, 13]. Consider the following example: SIR is a well-known model of disease spread in which the health state (Susceptible-Infected-Recovered) evolution of each person is described by a transition matrix M ; see Table 1 for an example. An important consideration for such a transition matrix M is what time length l is one time step [39]. Often, this time length l is fixed by experts (e.g., one day) and M estimated from repeated observation over these time intervals of length l . Thus, M captures the effect of “average” interaction (that enables disease spread) over this time interval. However, when applied for any population, the intensity of interaction can vary depending on various human factors such as norms (masking, etc.) and social events at that time. This has an effect that M might describe interaction over a time interval of length l' where l' is a random quantity dependent on group behavior. This results in a problem where the number of timesteps in a given time frame (e.g., one week) becomes uncertain. To handle the uncertainty, one may be interested in the worst case state of disease spread in a week in order to robustly estimate the cost of disease spread and make critical decisions about social distancing or masking. In a similar vein, such models are used to model attack propagation in cyber-security [6], where it is important to understand worst case outcomes and cost within a fixed wall clock time in order to take remedial actions. These issues motivate our theoretical work on a model of robustness in discrete time Markov chains and algorithmic approaches to robustly measure cost.

As far as we know, there is limited work studying the uncertainty of time horizon in discrete time linear dynamical systems. A typical approach to handle uncertainty is to introduce a single absorbing (or sink) state to indicate the end of the evolution of the system [14]. However, such approaches assume a known probability distribution over time horizon, sometimes learned from data, but do not handle uncertainty in the knowledge of such probability distribution from finitely many samples. Instead, we aim for robustness by forming uncertainty or ambiguity sets based on prior data samples (or expert inputs) of how many timesteps Markov chain could run in a given time frame.

Toward our goal, we first prove a fundamental result showing an equivalence between a discrete time Markov chain on a probability simplex and a global asymptotic stable (GAS) discrete time linear dynamical system. In particular, a GAS system satisfies some properties, such as Lyapunov stability (Definition 2.1), and converges to the zero vector $\mathbf{0}$. This convergence to $\mathbf{0}$ allows for easier notation and proof for our theory results for a GAS system and the equivalence provides an all-encompassing framework applicable for Markov chains without loss of generality (WLOG).

Next, we specify a robust cost estimation problem in a GAS system with an uncertain time horizon but given data samples of the number of time steps from past runs. We formulate this as a distributional problem with Wasserstein ambiguity set around a nominal distribution formed using the given time step samples. We call this the distributional robust cost estimation (DRCE) problem and a special case with unbounded ambiguity set is the robust cost estimation (RCE) problem. We consider two cases to solve: (1) finite support of the nominal distribution and (2) infinite support of the nominal distribution. We also show that our approach can jointly handle multiple uncertainties such additional uncertainty in the initial state.

We list all our contributions next: (1) A fundamental equivalence between a discrete time Markov Chain on a probability simplex and a GAS system. (2) A fast polynomial time algorithm (Algorithm 1) for evaluating the GAS state over finitely many time steps. (3) A detailed proof of the structure of Wasserstein-1 polytope on the probability simplex, resulting in a polynomial time solution for Wasserstein ambiguity set in the finite support case. (4) A hardness result for the infinite support case, and then a non-polynomial time algorithm for (RCE) problem and an approximation for the (DRCE) problem in this case. *All missing and full proofs are in Appendix A.*

Related Work. *Distributional Robustness:* A very widely studied topic in robust optimization literature [38], distributional robustness has recently found usage in machine learning [22, 12, 24], with applications in adversarial learning [33, 27, 23, 2], robust decision making [34, 5], and reinforcement learning [25, 32, 41]. Our work is situated in the same space but we do not solve a conventional distributional robust optimization [29], which involves choosing an action (or decision, or control or sometimes weight parameters). Here we perform distributional robust *estimation* of costs in the challenging situation of uncertain time horizon for a dynamically evolving state distribution.

Linear Dynamical Systems and Markov Chains: There are many works in linear dynamical systems, some recent ones focus on learning such systems [16, 30, 3, 35]. Markov chains have been used very widely in machine learning, such as in MCMC approaches [19] and other references in the introduction. Again, as stated in the introduction, different from any work that we know of, we aim for distributional robustness to tackle the uncertainty in time horizon.

2 Background and Preliminaries

We present basic notations and background in linear algebra, which can be found in textbooks [26]. We also present definitions for finite space and discrete time linear dynamical systems.

Notation: $[n]$ denotes $\{1, \dots, n\}$. We use bold notation, e.g., \mathbf{x} , to denote vectors. \mathbf{x}^\top is the transpose and $\dim(\mathbf{x})$ is the dimension of vector \mathbf{x} . \mathbf{e}_i denotes the i^{th} standard basis vector with 1 at position i and 0 elsewhere (dimension of the ambient space will be clear from context or mentioned if required), and $\mathbf{1} := \sum_i \mathbf{e}_i$. Denote $H_n := \{\mathbf{x} \in \mathbb{R}^n \mid \mathbf{1}^\top \mathbf{x} = 0\}$, $\Delta_n := \{\mathbf{x} \in \mathbb{R}^n \mid x_i \geq 0 \forall i \in [n], \mathbf{1}^\top \mathbf{x} = 1\}$ the probability simplex and $\overline{\Delta}_n := \{\mathbf{x} \in \mathbb{R}^n \mid \mathbf{1}^\top \mathbf{x} = 1\}$ the extended probability simplex which is the same as $H_n + \frac{1}{n}\mathbf{1}$. For a set $S \subseteq \mathbb{N}$, a distribution on S is a function $q : S \rightarrow [0, 1]$ such that $\sum_{s \in S} q(s) = 1$. These are the same as vectors $\mathbf{q} \in \mathbb{R}^S$ with non-negative entries that sum to 1. We will interchangeably use $q(s) = q_s$. The set of all distributions on S is denoted as $\Delta(S)$. M^\top denotes matrix M transpose and M_{ij} is the entry in row i and column j . $\rho(M)$ is the spectral radius of M , i.e., $\rho(M) = \max\{|\lambda_1|, \dots, |\lambda_n|\}$ for the n eigenvalues λ_i 's. I_n denotes the identity matrix of size

$n \times n$. Any complex number $a + ib$ can be written in Euler notation as $re^{i\theta} = r(\cos \theta + i \sin \theta)$, where $r = \sqrt{a^2 + b^2} \geq 0$ is the magnitude. Given non-zero b , we must have $\theta \in (0, \pi) \cup (\pi, 2\pi)$.

Real Jordan normal form: Any square matrix $M \in \mathbb{R}^{n \times n}$ can be written as $M = PJP^{-1}$ where $P \in \mathbb{R}^{n \times n}$, i.e., matrix with real valued entries, and J is a real valued matrix in Jordan form as described next. First, the eigenvalues of M can be complex or real valued. Complex eigenvalues appear in pairs, which we denote by $a + ib$ and $a - ib$. Suppose M has q pairs of complex eigenvalues and p real eigenvalues (q or p could be 0). Assume that the eigenvalues are distinct,¹ and the real ones are given by $\lambda_1 > \dots > \lambda_p$. For each complex pair of eigenvalues $a_j \pm ib_j$, define the Jordan block: $\begin{bmatrix} a_j & -b_j \\ b_j & a_j \end{bmatrix}$ or equivalently in the Euler notation as $r_j \begin{bmatrix} \cos \theta_j & -\sin \theta_j \\ \sin \theta_j & \cos \theta_j \end{bmatrix} = r_j J_j$. Then, the Jordan matrix J is a *block diagonal matrix* given as

$$J = \text{diag}(r_1 J_1, \dots, r_q J_q, \lambda_1, \dots, \lambda_p) \quad (1)$$

Matrix exponentiation takes a rather convenient form with Jordan form: $M^k = P J^k P^{-1}$, where J^k has the same structure as J : $J^k = \text{diag}(r_1^k J_1^k, \dots, r_p^k J_p^k, \lambda_1^k, \dots, \lambda_p^k)$. In particular, it is straightforward to check that $J_j^k = \begin{bmatrix} \cos k\theta_j & -\sin k\theta_j \\ \sin k\theta_j & \cos k\theta_j \end{bmatrix}$.

Discrete Time Linear Dynamical Systems. A discrete-time dynamical system on a metric space (X, d) is given by a function $f : X \rightarrow X$ which induces a sequence of points $\{\mathbf{x}, f(\mathbf{x}), f^2(\mathbf{x}), \dots\}$ in X starting from \mathbf{x} . A point $\mathbf{x}^* \in X$ is said to be an *equilibrium* or *fixed point* of f if $f(\mathbf{x}^*) = \mathbf{x}^*$.

Definition 2.1 (Globally Asymptotically Stable (GAS)). An equilibrium point \mathbf{x}^* is said to be *stable in the Lyapunov sense* for f if for every $\varepsilon > 0$ there is some $\delta_\varepsilon > 0$ such that $d(\mathbf{x}, \mathbf{x}^*) < \delta_\varepsilon$ implies $d(f^t(\mathbf{x}), \mathbf{x}^*) < \varepsilon$ for each integer $t \geq 0$. An equilibrium point \mathbf{x}^* is said to be *globally asymptotically stable* (GAS) if it is Lyapunov stable and $\lim_{t \rightarrow \infty} d(f^t(\mathbf{x}), \mathbf{x}^*) = 0$ for every $\mathbf{x} \in X$.

A special case of the above is a *discrete-time linear dynamical system* (DTLDS), in which we will consider $X \subset \mathbb{R}^n$ and f to be a linear map given by matrix $M \in \mathbb{R}^{n \times n}$ as $\mathbf{x}_{t+1} = M\mathbf{x}_t$. It is clear that a GAS system cannot have two equilibrium points in X . Also, for any norm $\|\cdot\|$ on \mathbb{R}^n a DTLDS is GAS with $\mathbf{x}^* = \mathbf{0}$ iff every eigenvalue of M has magnitude < 1 ($\rho(M) < 1$). We will usually take $\|\cdot\| = \|\cdot\|_1$ so that $d(\mathbf{x}, \mathbf{y}) = \|\mathbf{x} - \mathbf{y}\|_1$, unless stated otherwise.

One example of a GAS DTLDS which is *not on* \mathbb{R}^n but on the subspace Δ_n and is still described by a matrix is the well known concept of an *aperiodic irreducible Markov chain*. This system is described by a column stochastic matrix $M \in \mathbb{R}^{n \times n}$ with non-negative entries and each column summing to 1, and additional properties for irreducibility and aperiodicity [14]. It describes a dynamics on the probability simplex Δ_n because if $\mathbf{x} \in \Delta_n$ then $M\mathbf{x} \in \Delta_n$. It is known that $\exists! \boldsymbol{\pi} \in \Delta_n$ such that $M\boldsymbol{\pi} = \boldsymbol{\pi}$. This is the *stationary distribution* of the Markov chain and for any $\mathbf{x} \in \overline{\Delta}_n$ (note, not just Δ_n), $\lim_{t \rightarrow \infty} \|M^t \mathbf{x} - \boldsymbol{\pi}\|_1 = 0$. In this work, we consider GAS DTLDS systems for the core problem stated in Section 4. Our results apply to Markov chains WLOG, and we next relate GAS systems and Markov chains to support this claim.

3 GAS System and Markov Chain Relation

Consider an aperiodic irreducible Markov chain on Δ_n with transition matrix M . This M gives a GAS DTLDS on \mathbb{R}^{n-1} determined by $\overline{M} = AMB \in \mathbb{R}^{(n-1) \times (n-1)}$, where $B = \begin{bmatrix} \mathbf{0}^\top \\ -I_{n-1} \end{bmatrix} + \begin{bmatrix} I_{n-1} \\ \mathbf{0}^\top \end{bmatrix} \in \mathbb{R}^{n \times (n-1)}$ and $A \in \mathbb{R}^{(n-1) \times n}$ such that $A_{ij} = \begin{cases} 1 & \text{for } j \leq i \\ 0 & \text{otherwise} \end{cases}$. We will next show that for any $\mathbf{x}_0 \in \Delta_{n-1}$, the sequence of states $\mathbf{x}_1 = M\mathbf{x}_0, \mathbf{x}_2 = M\mathbf{x}_1, \dots$ converging to $\boldsymbol{\pi}$ is mirrored by the system \overline{M} . Before that, we show some structural relations.

Theorem 3.1 (Structural Relation). *For M and \overline{M} as defined above, we have (1) $B\overline{M} = MB$, (2) $\overline{M}Az = AMz$ for any $z \in H_n$, and (3) $\overline{M}^t = AM^tB$.*

In particular, the following corollary follows from the second property in the theorem above.

¹If two eigenvalues are same, perturb one by an arbitrarily small amount. See Appendix C for details.

Corollary 3.2. Let $\mathbf{v}_i := A(\mathbf{x}_i - \boldsymbol{\pi})$ for the sequence of states $\mathbf{x}_0, \mathbf{x}_1, \dots$ generated by M . Then, $\mathbf{v}_1 = \bar{M}\mathbf{v}_0, \mathbf{v}_2 = \bar{M}\mathbf{v}_1 \dots$ with the sequence converging to $\mathbf{0}$. We can recover \mathbf{x}_i from the system \bar{M} using $\mathbf{x}_i = B\mathbf{v}_i + \boldsymbol{\pi}$

This result above implies that we can obtain all the states in the dynamics of M starting from \mathbf{x}_0 by running the system \bar{M} starting from $A(\mathbf{x}_0 - \boldsymbol{\pi})$. A result similar to the above corollary but in the opposite direction (obtain states for \bar{M} by running M) can be obtained by leveraging the first property in Theorem 3.1. Finally, using the third property in Theorem 3.1, we prove the following:

Theorem 3.3. \bar{M} is a GAS system on \mathbb{R}^{n-1} with fixed point $\mathbf{0}$, hence all eigenvalues of \bar{M} have magnitude < 1 , i.e., $\rho(\bar{M}) < 1$.

4 Model and Problem Statement

Given a DTLDS with dynamics $\mathbf{x}_{t+1} = M\mathbf{x}_t$ starting at a fixed known \mathbf{x}_0 , we define a cost incurred when the system stops at a state \mathbf{x} . The cost $g(\mathbf{x}) = \langle \mathbf{c}, \mathbf{x} \rangle$ is defined as a linear function in \mathbf{x} given by constant vector \mathbf{c} . This is a natural cost for Markov chains, where \mathbf{x} is a probability distribution over underlying states and expected cost is \mathbf{x} -weighted average of the cost of each state. Following our analysis in the previous section, we can WLOG restrict our attention to GAS DTLDS only. This claim is supported by Corollary 3.2 whence for any Markov chain M , the cost $\langle \mathbf{c}, \mathbf{x} \rangle = \langle B^T \mathbf{c}, \mathbf{v} \rangle + \langle \mathbf{c}, \boldsymbol{\pi} \rangle$ where \mathbf{v} is a state of the corresponding GAS \bar{M} as previously defined; cost is again linear in \mathbf{v} . Thus, WLOG we let M be a GAS DTLDS and continue with using the notation \mathbf{x} for states.

The uncertainty in when the system stops is described by a probability distribution $\mathbf{p} = \{p_t\}_{t \in \mathcal{T}}$ over a set of consecutive times steps \mathcal{T} ($|\mathcal{T}|$ can be infinity); then, the overall expected reward is $\sum_{t \in \mathcal{T}} p_t \langle \mathbf{c}, \mathbf{x}_t \rangle$, where $\mathbf{x}_t = M^t \mathbf{x}_0$. Based on our motivation, we do not know the true \mathbf{p} but observe finitely many samples from the distribution. Given the samples, we can form an empirical distribution $\hat{\mathbf{p}} = \{\hat{p}_t\}_{t \in \mathcal{T}}$. Then, we consider an ambiguity set of distributions

$$\mathcal{P} = \{\mathbf{q} \in \Delta(\mathcal{T}) \mid W_1(\hat{\mathbf{p}}, \mathbf{q}) \leq \xi\}, \quad (2)$$

where W_1 is a Wasserstein-1 distance, which is a popular choice for ambiguity set in distributional robustness. In order to be robust, we consider the worst case cost over this ambiguity set, specified as the Distributional Robust Cost Estimation (DRCE) problem below. This takes a robust estimation form when ξ is large enough and \mathcal{P} is the entire probability simplex. In such a case, all dirac-delta distributions over \mathcal{T} are allowed and then due to the linear nature of the objective, the problem becomes Robust Cost Estimation (RCE) below. We aim to solve the problems DRCE and RCE.

$$\max_{\mathbf{q} \in \mathcal{P}} \sum_{t \in \mathcal{T}} q_t \langle \mathbf{c}, \mathbf{x}_t \rangle \quad (\text{DRCE}) \quad \mid \quad \max_{t \in \mathcal{T}} \langle \mathbf{c}, \mathbf{x}_t \rangle \quad (\text{RCE})$$

Remark: While our focus here is on temporal robustness, we can also handle additional uncertainty in the initial state \mathbf{x}_0 . More formally, let this uncertainty be specified by a set $\mathcal{U} = \{\mathbf{x} \mid \mathbf{x} = \hat{\mathbf{x}}_0 + \sum_{i=1}^U \alpha_i \mathbf{u}_i, \sum_{i=1}^U \alpha_i = 1, \alpha_i \geq 0 \forall i\}$ for given vertices $(\mathbf{u}_i)_{i \in [U]}$ (these vertices can arise in distributional ambiguity set, as we show in sequel for Wasserstein polytope) and a nominal $\hat{\mathbf{x}}_0$. The result below reduces the overall problem $\max_{\mathbf{x}_0 \in \mathcal{U}, \mathbf{q} \in \mathcal{P}} \sum_{t \in \mathcal{T}} q_t \langle \mathbf{c}, \mathbf{x}_t \rangle$ to solving DRCE U times. A similar result with RCE is a simple corollary of this result.

Proposition 4.1. $\max_{\mathbf{x}_0 \in \mathcal{U}, \mathbf{q} \in \mathcal{P}} \sum_{t \in \mathcal{T}} q_t \langle \mathbf{c}, \mathbf{x}_t \rangle = \max_{i \in [U]} \max_{\mathbf{q} \in \mathcal{P}} \sum_{t \in \mathcal{T}} q_t \langle \mathbf{c}, M^t(\hat{\mathbf{x}}_0 + \mathbf{u}_i) \rangle$

5 Approach

We describe our approach for finite and infinite support of $\hat{\mathbf{p}}$ in the two subsections next. Finite support arises when $\hat{\mathbf{p}}$ is the empirical distribution and infinite support when $\hat{\mathbf{p}}$ is an estimated parametric distribution, given data samples. WLOG and to avoid cumbersome notation, we assume that $\mathcal{T} = \{1, 2, \dots, T\} = [T]$, where T could be infinite.

5.1 Finite Support: Robust Cost Estimation

The naive way of solving the RCE problem is to evaluate $\langle \mathbf{c}, M^t \mathbf{x}_0 \rangle$ for each $t \in \mathcal{T}$. It is known that the dot product of two vectors (of size $\mathcal{O}(n)$) has $\mathcal{O}(n)$ time complexity, and the standard approach

Algorithm 1: Small and Big Strides (SaBS)

- 1 Let $B = \lfloor \sqrt{T} \rfloor$. Compute M^B by successive squaring (see text).
- 2 Preprocess M^B, M^\top, M as in [36].
- 3 Let $\mathbf{v}^j = M^j \mathbf{x}_0$. Compute $M^B \mathbf{x}_0, M^{2B} \mathbf{x}_0, \dots, M^{B^2} \mathbf{x}_0$ using $\mathbf{v}^{(i+1)B} = M^B \mathbf{v}^{iB}$.
- 4 Compute $(M^\top)^1 \mathbf{c}, (M^\top)^2 \mathbf{c}, \dots, (M^\top)^{B-1} \mathbf{c}$.
- 5 **for** each $t \in \{1, \dots, B^2\}$ **do**
- 6 | Obtain $\langle \mathbf{c}, M^t \mathbf{x}_0 \rangle = \langle (M^\top)^{t \bmod B} \mathbf{c}, M^{\lfloor t/B \rfloor B} \mathbf{x}_0 \rangle$ using precomputed values above.
- 7 **for** each t iterating over $\{B^2 + 1, \dots, T\}$ **do**
- 8 | Compute $M^t \mathbf{x}_0 = M \mathbf{v}^{t-1}$, and then $\langle \mathbf{c}, M^t \mathbf{x}_0 \rangle$. Let $\mathbf{v}^t = M^t \mathbf{x}_0$.
- 9 **Output:** All $\langle \mathbf{c}, M^t \mathbf{x}_0 \rangle$ for $t \in \mathcal{T}$.

of n dot products to compute a matrix-vector product has $\mathcal{O}(n^2)$ time complexity. Using the fact that $M^t \mathbf{x}_0 = M \times M^{t-1} \mathbf{x}_0$, a naive approach would require T matrix-vector and T dot products yielding a time complexity of $\mathcal{O}(n^2 T)$.

A slightly better approach can be obtained by observing that $M^t \mathbf{x}_0 = M \times M^{t-1} \mathbf{x}_0$ involves multiplying the same matrix M with different vectors. A prior result [36] has shown that by preprocessing the matrix M , the time complexity of T matrix-vector products is $\mathcal{O}(n^{2+\varepsilon} + Tn^2/(\varepsilon \log n)^2)$ for any constant ε . Thus, if T is larger than n , then the preprocessing step of $\mathcal{O}(n^{2+\varepsilon})$ can be beneficial.

We take this approach further in an algorithm that we call Small and Big Strides (SaBS) shown in Algorithm 1. We start with the observation that $\langle \mathbf{c}, M^t \mathbf{x}_0 \rangle = \langle M^\top \mathbf{c}, M^{t-1} \mathbf{x}_0 \rangle$, and applying this recursively $\langle \mathbf{c}, M^t \mathbf{x}_0 \rangle = \langle (M^\top)^j \mathbf{c}, M^{t-j} \mathbf{x}_0 \rangle$. Let $B = \lfloor \sqrt{T} \rfloor$. First, we compute M^B (line 2) by successive squaring M^1, M^2, M^4 , a popular approach in number theory [21]. Then, preprocess M^B, M^\top and M for later use in multiple matrix-vector products. Then, precompute $M^B \mathbf{x}_0, M^{2B} \mathbf{x}_0, \dots, M^{B^2} \mathbf{x}_0$ and $(M^\top)^1 \mathbf{c}, \dots, (M^\top)^{B-1} \mathbf{c}$. Then, using the fact that $\langle \mathbf{c}, M^t \mathbf{x}_0 \rangle = \langle (M^\top)^{t \bmod B} \mathbf{c}, M^{\lfloor t/B \rfloor B} \mathbf{x}_0 \rangle$, we can compute all $\langle \mathbf{c}, M^t \mathbf{x}_0 \rangle$ for each $t \in \{1, \dots, B^2\}$ using the precomputed values in the loop at line 6. The remaining powers from $B^2 + 1$ to T is computed in loop starting at line 7. We achieve a better runtime dependence on T :

Lemma 5.1. *The time complexity of SaBS is $\mathcal{O}(n^\omega \log T + n^{2+\varepsilon} + \sqrt{T}n^2/(\varepsilon \log n)^2 + nT)$, where n^ω is the time complexity of matrix multiplication. (best known ω currently is ≈ 2.3715 [37]).*

The result above improves the dominating term $Tn^2/(\varepsilon \log n)^2$ from the previous approach to $\sqrt{T}n^2/(\varepsilon \log n)^2$ and introduces the terms nT that is better than $Tn^2/(\varepsilon \log n)^2$. Also, for T larger than n , the term $n^\omega \log T$ is better than $Tn^2/(\varepsilon \log n)^2$. As a final remark, another plausible approach is to find the real Jordan form of $M = PJP^{-1}$ and use the fact that $M^k = PJ^kP^{-1}$. We show in Appendix C that this plausible approach has worse time complexity than above.

5.2 Finite Support: Distributional Robust Cost Estimation

Wasserstein ambiguity sets have been applied in optimization and machine learning in [22, 28]. First, we present a useful and general geometric characterization of Wasserstein distance in finite dimension that has appeared in recent literature [7, 8, 10] without a detailed proof, thus, we provide a detailed proof of the characterization. Fix a distance $d : \mathcal{T} \times \mathcal{T} \rightarrow \mathbb{R}_{\geq 0}$. This is essentially given by a symmetric matrix with entries d_{ij} such that $d_{ii} = 0 \forall i \in \mathcal{T}$, $d_{ij} > 0$ whenever $i \neq j \in \mathcal{T}$, and $d_{ij} + d_{jk} \geq d_{ik} \forall i, j, k \in \mathcal{T}$. The Wasserstein distance $W^d(\boldsymbol{\rho}, \boldsymbol{\nu}) = W_1^d(\boldsymbol{\rho}, \boldsymbol{\nu})$ based on the metric (d_{ij}) between two probability distributions $\boldsymbol{\rho}, \boldsymbol{\nu} \in \Delta(\mathcal{T})$ is defined for finite \mathcal{T} in a dual form as

$$\max \left\{ \sum_{i=1}^T (\rho_i - \nu_i) x_i \mid |x_i - x_j| \leq d_{ij} \forall i, j \in \mathcal{T} \right\}.$$

The above definition is a direct result of Kantorovich duality, e.g., used in Wasserstein GAN [1]. Recall that any norm $\|\cdot\|$ in a vector space X is a function that satisfies certain properties for any $x, y \in X$: (1) triangle inequality: $\|x + y\| \leq \|x\| + \|y\|$ (2) absolute homogeneity: $\|ax\| = |a| \|x\|$, and (3) positivity: $\|x\| = 0$ iff $x = 0$. Recall H_T , which was defined as $\{\mathbf{x} \in \mathbb{R}^T \mid \mathbf{1}^\top \mathbf{x} = 0\}$, is a subspace of \mathbb{R}^T . Then, the Wasserstein distance W_1^d induces a norm on H_T :

Proposition 5.2. *The following is a norm on H_T :*

$$\|\boldsymbol{\mu}\|_W^d := \max \{ \boldsymbol{\mu}^\top \mathbf{x} \mid \mathbf{x} \in \mathbb{R}^T, |x_i - x_j| \leq d_{ij} \forall i, j \}.$$

Observe that the constraint set of the above linear program is unbounded, that is, if \mathbf{x} satisfies the constraints, then so does $\mathbf{x} + \lambda \mathbf{1}$ for any real number λ and also, given $\boldsymbol{\mu} \in H_T$, $\boldsymbol{\mu}^\top (\mathbf{x} + \lambda \mathbf{1}) = \boldsymbol{\mu}^\top \mathbf{x}$. This observation allows for an equivalent formulation further restricting \mathbf{x} to a bounded set

$$\|\boldsymbol{\mu}\|_W^d = \max \{ \boldsymbol{\mu}^\top \mathbf{x} \mid \mathbf{x} \in H_T, |x_i - x_j| \leq d_{ij} \forall i, j \}.$$

Next, recall that our ambiguity set \mathcal{P} in Equation 2 contain $\mathbf{q} \in \Delta_T$ such that $W_1^d(\hat{\mathbf{p}}, \mathbf{q}) \leq \varepsilon$. From the definition of W_1^d above and the norm, we can see that this is the same as $\|\boldsymbol{\mu}\|_W^d \leq \xi$ for $\boldsymbol{\mu} = \mathbf{q} - \hat{\mathbf{p}}$. Further, since $q_i \geq 0$, this straightforwardly leads to following conclusion:

$$\mathcal{P} = \{ \mathbf{q} \mid \mathbf{q} = \hat{\mathbf{p}} + \boldsymbol{\mu}, \boldsymbol{\mu} \in H_T, \|\boldsymbol{\mu}\|_W^d \leq \xi, \mathbf{q} \geq 0 \}$$

Alternatively, the above can be thought of as the intersection of the probability simplex Δ_T and the norm ball $\|\boldsymbol{\mu}\|_W^d \leq \xi$ shifted by $\hat{\mathbf{p}}$. An illustration in 3-d is shown in Figure 1. Thus, we investigate the structure of the norm $\|\cdot\|_W^d$. We show that the unit ball of this norm is a $T - 1$ dimensional polytope.

Theorem 5.3. *The Wasserstein unit ball in H_T around the origin $\mathbf{0} \in \mathbb{R}^T$ based on the distance $d : \mathcal{T}^2 \rightarrow \mathbb{R}_{\geq 0}$ is the convex hull of the points $\left\{ \frac{\mathbf{e}_i - \mathbf{e}_j}{d_{ij}} \mid i \neq j \right\}$.*

Proof Sketch. For the Wasserstein ball of radius 1 around $\mathbf{0} \in \mathbb{R}^T$, we want to find those $\boldsymbol{\mu} \in H_T$ such that $\boldsymbol{\mu}^\top \mathbf{x} \leq 1$ for every $\mathbf{x} \in H_T$ satisfying $A\mathbf{x} \leq \mathbf{1}, \mathbf{1}^\top \mathbf{x} \leq 0, -\mathbf{1}^\top \mathbf{x} \leq 0$, where A is the matrix whose rows comprise of the constraint vectors $\frac{\mathbf{e}_i - \mathbf{e}_j}{d_{ij}}$. Then, following a number of algebraic steps and using Farkas lemma, we get that $\boldsymbol{\mu} = A^\top \boldsymbol{\lambda}$ for $\mathbf{1}^\top \boldsymbol{\lambda} = 1, \boldsymbol{\lambda} \geq 0$. A typical column of A^\top looks like $\frac{\mathbf{e}_i - \mathbf{e}_j}{d_{ij}}$, which gives us the desired result. \blacksquare

Following from the general result above, for our problem d_{ij} represent distance between time points on the line. It is natural to thus consider the distance function to be given by $d_{ij} = |i - j|$. Then, the set of corners proposed in the above theorem are $T(T - 1)$ in number. However, a further observation with the mentioned distance function yields that if $s < t \in [T]$ then $\mathbf{v}_{st} = \frac{\mathbf{e}_t - \mathbf{e}_s}{d_{st}} = \frac{1}{t-s} \sum_{k=s}^{t-1} (\mathbf{e}_{k+1} - \mathbf{e}_k) = \frac{1}{t-s} \sum_{k=s}^{t-1} \mathbf{v}_{k+1, k}$ and similar if $s > t$. This implies that \mathbf{v}_{st} for $|s - t| > 1$ cannot be an extreme point of the polytope as it is a convex combination of other extreme points. Thus, there are only $2(T - 1)$ extreme points of the Wasserstein unit ball polytope, namely $\pm \mathbf{v}_{1,2}, \dots, \pm \mathbf{v}_{T-1,T}$. For the ξ Wasserstein ball polytope, these extreme points will be just multiplied by ξ . As a consequence, using conv to denote convex hull, we can write

$$\mathcal{P} = \{ \mathbf{q} \mid \mathbf{q} = \hat{\mathbf{p}} + \boldsymbol{\mu}, \boldsymbol{\mu} \in \text{conv}(\pm \xi \mathbf{v}_{1,2}, \dots, \pm \xi \mathbf{v}_{T-1,T}), \mathbf{q} \geq 0 \}.$$

Recall that DRCE is a linear program (LP) with the constraint as \mathcal{P} . Then, there are two cases.

Case 1: $\hat{\mathbf{p}} + \boldsymbol{\mu} \in \Delta_T \forall \boldsymbol{\mu} \in \text{conv}(\pm \xi \mathbf{v}_{1,2}, \dots, \pm \xi \mathbf{v}_{T-1,T})$. This case is illustrated by the polytope with center D in Figure 1. An LP has optimum at one of the extreme points of its constraint set. Hence, while solving an LP on this polytope, one needs to compute the objective value of the program only at the $\mathcal{O}(T)$ extreme points. In other words, when optimizing over \mathcal{P} , where ξ is small enough to make each extreme points $\hat{\mathbf{p}} \pm \xi(\mathbf{e}_i - \mathbf{e}_{i+1}) \in \Delta(T)$ for $i \in [T - 1]$, we only have to evaluate the objective at these extreme points and choose the maximum of the evaluated values. Noting the similarity of this to the robust estimation case, and from Lemma 5.1, it is straightforward to check that the runtime is $\mathcal{O}(n^\omega \log T + n^{2+\varepsilon} + \sqrt{Tn^2}/(\varepsilon \log n)^2 + nT)$.

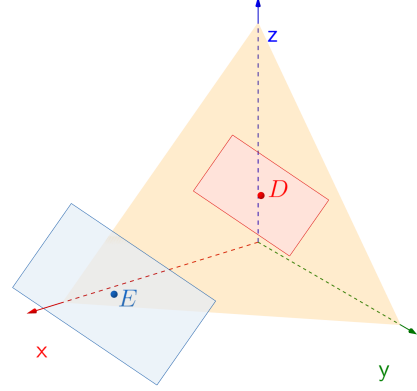


Figure 1: $\|\cdot\|_W^d$ ($d_{ij} = |i - j|$) balls on the probability simplex with $\xi = 0.3$ centered at $E = (0.83, 0.13, 0.04)$ and $\xi = 0.2$ centered at $D = (0.24, 0.35, 0.41)$.

Case 2: For some $\mu \in \text{conv}(\pm \xi \mathbf{v}_{1,2}, \dots, \pm \xi \mathbf{v}_{T-1,T})$, $\hat{\mathbf{p}} + \mu \notin \Delta_T$. This case is illustrated by the polytope with center E in Figure 1. In this case the number of extreme points can be large, but we can write this problem as an LP as follows:

$$\begin{aligned} \max_{\mathbf{q} \in \mathbb{R}^T, \lambda_i \in \mathbb{R}} \quad & \sum_{t \in \mathcal{T}} q_t \langle \mathbf{c}, \mathbf{x}_t \rangle \quad \text{s.t.} \quad \mathbf{q} \geq 0, \quad \sum_i \lambda_i = 1, \quad \lambda_i \geq 0 \quad \forall i, \\ & \mathbf{q} = \hat{\mathbf{p}} + \lambda_1 \xi \mathbf{v}_{1,2} + \dots + \lambda_{T-1} \xi \mathbf{v}_{T-1,T} + \lambda_T (-\xi \mathbf{v}_{1,2}) + \dots + \lambda_{2(T-1)} (-\xi \mathbf{v}_{T-1,T}). \end{aligned} \quad (3)$$

The above LP has $\mathcal{O}(T)$ number of optimization variables, and is represented in L bits, where L is $\mathcal{O}(T)$ assuming a fixed number of bits for each constant and variable. Then, an LP requires $\mathcal{O}(n^{3.5} L^2)$ time for solving exactly, which can be improved to $\mathcal{O}(n^{3.5} L)$ runtime if we allow for any arbitrary approximation [20]. Note that we also need to compute the $\langle \mathbf{c}, \mathbf{x}_t \rangle$ for all $t \in \mathcal{T}$, which is the same as robust estimation case. Thus, considering the dominating terms, we obtain an overall complexity of $\mathcal{O}(n^{3.5} T^2)$ in the exact case and $\mathcal{O}(n^{3.5} T)$ with arbitrary approximation.

5.3 Infinite Support: Robust Cost Estimation

With an infinite \mathcal{T} , the methods developed till now do not apply as they require computing over $|\mathcal{T}|$ steps. Thus, we explore a different set of methods for the infinite case. Assume $M = PJP^{-1}$ where J is in its reduced real Jordan form in Equation 1. WLOG let these blocks be ordered such that $r_1 < \dots < r_q$ and $|\lambda_1| < \dots < |\lambda_p|$. We also know that all these magnitudes are strictly less than one ($r_i, |\lambda_j| < 1$) as our problem statement handles GAS systems. As stated after Equation 1,

$J^t = \text{diag}(r_1^t J_1^t, \dots, \lambda_p^t)$ where the i^{th} 2×2 block $J_i^t = r_i^t \begin{bmatrix} \cos t\theta_i & -\sin t\theta_i \\ \sin t\theta_i & \cos t\theta_i \end{bmatrix}$. We consider $\langle \mathbf{c}, P J^t P^{-1} \mathbf{x} \rangle$ as a function of t which is $\sum_{i=1}^q r_i^t (u_i \cos t\theta_i - v_i \sin t\theta_i) + \sum_{j=1}^p w_j \lambda_j^t$ where u_i, v_i, w_j only depend on $\mathbf{c}, \mathbf{x}, P$ (details in Appendix C). Let $(u_i, v_i) = (d_i \cos \eta_i, d_i \sin \eta_i)$ where $\eta_i \in [0, 2\pi)$ and $d_i = \sqrt{u_i^2 + v_i^2}$. So the expression we consider is

$$g(t) = \langle \mathbf{c}, P J^t P^{-1} \mathbf{x} \rangle = \sum_{i=1}^q d_i r_i^t \cos(t\theta_i + \eta_i) + \sum_{j=1}^p w_j \lambda_j^t.$$

Note that the RCE problem here is to solve $\max_{t \in \mathbb{N}} g(t)$.

Main Approach: Our approach here is to find a t_0 such that $g(t_0) > 0$. Then, since our problem is for a GAS system with $r_i, |\lambda_j| < 1$, we know that $g(t)$ converges to 0 as $t \rightarrow \infty$. Thus, from basic real analysis, there must exist a n_0 such that $\forall t' > n_0, |g(t')| < g(t_0)$. Our approach is to compute $g(t)$ for $t = 1$ to n_0 and choose the maximum among these. We show a construction of n_0 next.

Proposition 5.4. For any positive integer n_0 more than $\left\lceil \log_{\zeta} \frac{g(t_0)}{\sum |d_i| + \sum |w_j|} \right\rceil$, where $\zeta := \max \{|\lambda_p|, r_q\}$, we have $|g(t')| < g(t_0) \forall t' > n_0$.

The correctness of the approach is straightforward. Since we already found t_0 with $g(t_0) > 0$ and $g(t') < g(t_0)$ beyond n_0 (note that $n_0 \geq t_0$ is implied), then any time step t^* for which $g(t^*)$ is maximum must be such that $1 \leq t^* \leq n_0$. Also, there is a special case when there is no such t_0 that can be found, and then g takes maximum value at ∞ . Next, we explain how to find such a t_0 or infer that there is no such t_0 . We consider two cases.

Case 1: $r_q < |\lambda_p|$. Then $w_p \lambda_p^t$ is the dominating term in g . Dividing $g(t)$ by $|\lambda_p|^t$ we obtain $\frac{g(t)}{|\lambda_p|^t} = \sum_{i=1}^q d_i \left(\frac{r_i}{|\lambda_p|} \right)^t \cos(t\theta_i + \eta_i) + \sum_{j=1}^{p-1} w_j \left(\frac{\lambda_j}{|\lambda_p|} \right)^t + w_p (\text{sgn } \lambda_p)^t$. Then, we show that:

Proposition 5.5. $\left| \frac{g(t)}{|\lambda_p|^t} - w_p (\text{sgn } \lambda_p)^t \right| \leq \beta \varepsilon^t$ with $\beta := \sum_{i=1}^q |d_i| + \sum_{j=1}^{p-1} |w_j|$ and $\varepsilon := (\max\{r_1, \dots, r_q, |\lambda_1|, \dots, |\lambda_{p-1}|\}) / |\lambda_p| < 1$.

In the following, we show how to find t_0 .

Lemma 5.6. For the three cases below, we state a cutoff beyond which we can find t_0 :

- $w_p > 0, \lambda_p > 0 : \forall t > \log_{\varepsilon} \left(\frac{w_p}{\beta} \right), g(t) > 0$. Thus, $t_0 = 1 + \max \{ \lceil \log_{\varepsilon} \left(\frac{w_p}{\beta} \right) \rceil, 1 \}$.
- $w_p > 0, \lambda_p < 0 : \forall t > \frac{1}{2} \log_{\varepsilon} \left(\frac{w_p}{\beta} \right), g(2t) > 0$. Thus, $t_0 = 2 + 2 \max \{ \lceil \frac{1}{2} \log_{\varepsilon} \left(\frac{w_p}{\beta} \right) \rceil, 1 \}$.

- $w_p < 0, \lambda_p < 0 : \forall t > \frac{1}{2} \log_\varepsilon \left(\frac{-w_p}{\beta} \right), g(2t+1) > 0$. Thus, $t_0 = 2 \max \left\{ \left\lceil \frac{1}{2} \log_\varepsilon \left(\frac{-w_p}{\beta} \right) \right\rceil, 1 \right\} + 1$.

Finally, for the remaining case of $w_p < 0, \lambda_p > 0, \forall t > \log_\varepsilon \left(\frac{-w_p}{\beta} \right), g(t) < 0$. Hence, search for some $1 \leq n_0 \leq \lfloor \log_\varepsilon \left(\frac{-w_p}{\beta} \right) \rfloor$ for which $g(n_0)$ is positive and is maximized. If the search returns empty, then no such n_0 exists for this last case. Here ε, β are as in Proposition 5.5.

Case 2: $r_q > |\lambda_p|$. Similar to case 1, we consider $\frac{g(t)}{r_q^t} = \sum_{i=1}^{q-1} d_i \left(\frac{r_i}{r_q} \right)^t \cos(t\theta_i + \eta_i) + \sum_{j=1}^p w_j \left(\frac{\lambda_j}{r_q} \right)^t + d_q \cos(t\theta_q + \eta_q)$. Then, we show that

Proposition 5.7. $\left| \frac{g(t)}{r_q^t} - d_q \cos(t\theta_q + \eta_q) \right| \leq \gamma C^t$ with $\gamma := \sum_{i=1}^{q-1} |d_i| + \sum_{j=1}^p |w_j|, C := (\max\{r_1, \dots, r_{q-1}, |\lambda_1|, \dots, |\lambda_p|\})/r_q < 1$.

If we measure angles in degrees (to avoid irrationality of π) we can show the following form for t_0 .

Lemma 5.8. Given angles are measured in degrees and $\theta_q = a/b \in \mathbb{Q}$ with $a, b \in \mathbb{Z}_{>0}$ and $\gcd(a, b) = 1$, there exist integers $n \neq 0, l$ such that $an + 360bl = \gcd(360, a) = g$, computable in $\mathcal{O}(\log(\min(a, b)))$. Let C, d_q, γ be as in Proposition 5.7. Then, for any integer $p \in (0, 90b)$, t_0 is

$$(n(p - bc) + |n| (s_0 + \max\{1, \lceil D \rceil\})360b)/g, \text{ where}$$

$$s_0 = 1 + \max \left\{ 0, \left\lceil \frac{\text{sgn}(n)(cb-p)}{360} \right\rceil \right\}, D + s_0 = \frac{g \log_C \left(\frac{|d_q|}{2\gamma} \right) - n(p-cb)}{360b|n|} \text{ and } c = 135 + \lfloor \eta \rfloor - \text{sgn}(d_q) \cdot 90.$$

Hardness: The above results show that the steps required depend on the input problem, and can be arbitrarily large (e.g., for ζ nearly 1 in Prop. 5.4). Indeed, the next NP Hardness result shows that the RCE problem for infinite support is not easy in general, unless $P = NP$.

Theorem 5.9. Given $n \in \mathbb{N}, M \in \mathbb{Q}^{n \times n}$ with $\rho(M) < 1, \mathbf{a} \in \mathbb{Q}^n, \mathbf{c} \in \mathbb{Q}^n, \alpha \in \mathbb{Q}$, it is NP-hard to decide whether there exists $t \in \mathbb{N}$ such that $\langle \mathbf{c}, M^t \mathbf{a} \rangle > \alpha$.

Given the above, unsurprisingly, the lemma below shows that there exists instances for which the RCE problem for infinite support is not easy following our approach. We show tighter results for the special case of $n = 2$ in Appendix B.

Lemma 5.10. $\forall k, \exists \mathbf{c}_k, \mathbf{x}_k \in \mathbb{R}^n, M_k \in \mathbb{R}^{n \times n}$ with $\rho(M_k) < 1$ s.t. $\inf\{t \in \mathbb{N} \mid \langle \mathbf{c}_k, M_k^t \mathbf{x}_k \rangle > 0\} \geq k$.

5.4 Infinite Support: Distributional Robust Cost Estimation

The hardness result already shows that the DRCE problem is hard, as RCE is a special case of DRCE. In fact, note that representing the distribution $\hat{\mathbf{p}}$ over infinite support is possible on a computer only as a parametric distribution. Here, noting that a geometric distribution with parameter ρ captures the first occurrence of an event, we show results for distributions represented by geometric distribution with the success event indicating the stoppage of the GAS system. Let $\hat{\rho}$ be the parameter for $\hat{\mathbf{p}}$, and we restrict the distributions in the ambiguity set of Equation 2 to be from the geometric family, thus, we write \mathbf{q}_ρ to indicate the parameter ρ for any $\mathbf{q} \in \mathcal{P}$. By geometric distribution $q_\rho(t) = (1 - \rho)^{t-1} \rho$. Then, from standard results [9], we get $W_1(\mathbf{q}_\rho, \hat{\mathbf{p}}) = |1/\rho - 1/\hat{\rho}|$, which further implies the restriction that $\frac{\hat{\rho}}{1+\hat{\rho}\xi} \leq \rho \leq \frac{\hat{\rho}}{1-\hat{\rho}\xi}$. Then, using the fact that $g(t)$ converges to $\mathbf{0}$, we can choose a n_0 and optimize for $\sum_{t=1}^{n_0} g(t)q_\rho(t)$ to obtain the following arbitrary additive approximation.

Proposition 5.11. Let $n_0 = \lceil \log_\zeta \frac{\varepsilon}{\sum |d_i| + \sum |w_j|} \rceil$, where $\zeta = \max \{|\lambda_p|, r_q\}$, for small ε . Let $\delta = (1 - \rho)^{n_0}$, then $|\sum_{t=1}^{\infty} g(t)q_\rho(t) - \sum_{t=1}^{n_0} g(t)q_\rho(t)| \leq \varepsilon \delta$.

We note that $\sum_{t=1}^{n_0} g(t)q_\rho(t)$ may be a non-convex function in ρ and we can use projected gradient ascent with random restarts to aim to find the maximum. Similar results can be obtained for other parametric distributions, such as Poisson or negative binomial, that admit a closed form formula for Wasserstein-1 distance in terms of the parameters.

6 Experiments

While our work is mainly theoretical in nature, we provide some experiments supporting the theory. In the main paper, we focus on two experiments: (1) synthetic experiments showing

Table 1: SIR Transitions

From	to S	to I	to R
S	0.2	0.8	0
I	0	0.5	0.5
R	0.1	0	0.9

Table 2: SVIR Transitions

From	to S	to V	to I	to R
S	0.1	0.1	0.8	0
V	0.1	0.9	0	0
I	0	0	0.5	0.5
R	0.1	0	0	0.9

Table 3: Solution Characteristics

Characteristic	SIR	SVIR
Emp. Cost \hat{C}	0.75	0.69
%> \hat{C}	56	54
DRCE Cost C	1.96	1.03
%> C	23	15

how our approach scales with state space and (2) disease spread modeling using numbers taken from [11]. Additional experiments showing computational advantage of converting a Markov Chain to GAS system (Section 3) and a possible use case for our approach are in Appendix D. All experiments were run on Apple M2 Chip with 8 CPUs over 2.4 GHz each and 8GB RAM. Our synthetic experiments are for the RCE problem with an uncertain time horizon $\mathcal{T} = [T] = [10000]$. The results are based on runs of the SaBS algorithm and a baseline naive approach (Section 5.1) on 30 randomly generated input matrices M of a given size $2^N \times 2^N$. We increase the size of N , with a cutoff of the model size that runs within an hour. Figure 2 shows the runtime (in log scale of seconds) against N . The results show a SaBS can handle large state space and large T on a regular laptop much better than the naive approach.

Our experiments based on transition matrix numbers from [11] model a SIR disease spread within five people. We add a vaccinated state to model SVIR disease spread and compare the vaccinated vs non-vaccinated scenario. The transitions are shown in Table 1 and 2. The full Markov chain states describe the joint state of all individuals (e.g., SSSSS means all five are Susceptible). We associate a cost of 1 with Infected, and 0 otherwise, e.g., state SIIIS has a cost of 2. We assume that everyone is Susceptible initially for the SIR model and considering practicalities such as vaccine hesitancy, 40% of the population is Susceptible and 60% Vaccinated initially for the SVIR model. We are interested in understanding the cost after 8 days, which nominally suggests that we should take 8 timesteps in the Markov chain. However, based on our motivation, we assume that the number of timesteps could vary from 1 to 15 with mean as 8.

We generate 100 samples of number of steps times from a binomial distribution with mean as 8 and range from 1-15. We form an empirical distribution \hat{p} from these samples and solve for DRCE with a Wasserstein ball of size $\xi = 2$ around the empirical distribution to get the DRCE *expected cost* C . Also, we solve the problem classically, by just assuming a running time of 8 timesteps and obtain an *empirical expected cost* \hat{C} . These numbers are shown in Table 3. Also, we ran the chain (sample states and run) 100 times, each for a number of the timesteps as present in our sampled timesteps. At the end of this run, we record the cost as given by the final state. Thus, we obtain 100 possible values of costs. We then estimate how likely is it that the true costs will exceed C and \hat{C} , by calculating the percentage of the 100 costs from the 100 runs that lie above these costs. These numbers are in Table 3. As expected, DRCE solution cost is more conservative and the chance of actual cost exceeding C is smaller than that for \hat{C} ; this allows for more robust decision making. Also, the DRCE solution shows a bigger difference in cost C between the SIR and SVIR cases, which reveals that DRCE can bring out the difference between vaccinating or not more starkly and with higher confidence.

7 Conclusion

We proposed a pertinent distributional robust cost estimation problem in GAS systems with uncertain time horizon, and presented theoretical results to solve it that also yielded fundamental general theory results. A number of promising research directions can be pursued, such as exploring different ambiguity sets, time horizon robustness in control problems, approximation algorithm for the NP-Hard case, and uncertainty in other problem parameters.

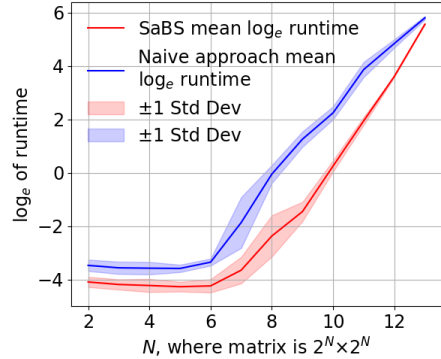


Figure 2: Runtime over 30 random instance with varying size.

References

- [1] Martin Arjovsky, Soumith Chintala, and Léon Bottou. Wasserstein generative adversarial networks. In *International conference on machine learning*, pages 214–223. PMLR, 2017.
- [2] Xingjian Bai, Guangyi He, Yifan Jiang, and Jan Oblój. Wasserstein distributional robustness of neural networks. *Advances in Neural Information Processing Systems*, 36, 2024.
- [3] Ainesh Bakshi, Allen Liu, Ankur Moitra, and Morris Yau. Tensor decompositions meet control theory: Learning general mixtures of linear dynamical systems. In Andreas Krause, Emma Brunskill, Kyunghyun Cho, Barbara Engelhardt, Sivan Sabato, and Jonathan Scarlett, editors, *Proceedings of the 40th International Conference on Machine Learning*, volume 202 of *Proceedings of Machine Learning Research*, pages 1549–1563. PMLR, 23–29 Jul 2023.
- [4] Vincent D. Blondel and Natacha Portier. The presence of a zero in an integer linear recurrent sequence is np-hard to decide. *Linear Algebra and its Applications*, 351-352:91–98, 2002. Fourth Special Issue on Linear Systems and Control.
- [5] Avinandan Bose, Arunesh Sinha, and Tien Mai. Scalable distributional robustness in a class of non-convex optimization with guarantees. *Advances in Neural Information Processing Systems*, 35:13826–13837, 2022.
- [6] Rodrigo Matos Carnier, Yue Li, Yasutaka Fujimoto, and Junji Shikata. Exact markov chain of random propagation of malware with network-level mitigation. *IEEE Internet of Things Journal*, 10(12):10933–10947, 2023.
- [7] Türkü Özlüm Çelik, Asgar Jammeshan, Guido Montúfar, Bernd Sturmfels, and Lorenzo Venturello. Optimal transport to a variety. In Daniel Slamanig, Elias Tsigaridas, and Zafeirakis Zafeirakopoulos, editors, *Mathematical Aspects of Computer and Information Sciences*, pages 364–381, Cham, 2020. Springer International Publishing.
- [8] Türkü Özlüm Çelik, Asgar Jammeshan, Guido Montúfar, Bernd Sturmfels, and Lorenzo Venturello. Wasserstein distance to independence models. *Journal of symbolic computation*, 104:855–873, 2021.
- [9] Marco De Angelis and Ander Gray. Why the 1-wasserstein distance is the area between the two marginal cdfs. *arXiv preprint arXiv:2111.03570*, 2021.
- [10] Greg DePaul, Serkan Hoşten, Nilava Metya, and Ikenna Nomesa. Degrees of the wasserstein distance to small toric models. *Algebraic Statistics*, 2024.
- [11] Emmanuel F. Drabo and William V. Padula. 264introduction to markov modeling. In *Handbook of Applied Health Economics in Vaccines*. Oxford University Press, 02 2023.
- [12] John Duchi and Hongseok Namkoong. Variance-based regularization with convex objectives. *Journal of Machine Learning Research*, 20(68):1–55, 2019.
- [13] Christian Dudel and Mikko Myrskylä. Estimating the number and length of episodes in disability using a markov chain approach. *Population Health Metrics*, 18:1–9, 2020.
- [14] David Freedman. *Markov chains*. Springer Science & Business Media, 2012.
- [15] Yi Hao, Alon Orlitsky, and Venkatadheeraj Pichapati. On learning markov chains. *Advances in Neural Information Processing Systems*, 31, 2018.
- [16] Elad Hazan, Holden Lee, Karan Singh, Cyril Zhang, and Yi Zhang. Spectral filtering for general linear dynamical systems. *Advances in Neural Information Processing Systems*, 31, 2018.
- [17] Ronald A Howard. *Dynamic Probabilistic Systems, Volume I: Markov Models*, volume 1. Courier Corporation, 2012.
- [18] Brooke E Husic and Vijay S Pande. Markov state models: From an art to a science. *Journal of the American Chemical Society*, 140(7):2386–2396, 2018.

[19] Galin L Jones and Qian Qin. Markov chain monte carlo in practice. *Annual Review of Statistics and Its Application*, 9(1):557–578, 2022.

[20] Narendra Karmarkar. A new polynomial-time algorithm for linear programming. In *Proceedings of the sixteenth annual ACM symposium on Theory of computing*, pages 302–311, 1984.

[21] Alan H Karp. Exponential and logarithm by sequential squaring. *IEEE transactions on computers*, 100(5):462–464, 1984.

[22] Daniel Kuhn, Peyman Mohajerin Esfahani, Viet Anh Nguyen, and Soroosh Shafieezadeh-Abadeh. *Wasserstein distributionally robust optimization: Theory and applications in machine learning*, pages 130–166. INFORMS, 10 2019.

[23] Aounon Kumar, Alexander Levine, Tom Goldstein, and Soheil Feizi. Provable robustness against wasserstein distribution shifts via input randomization. In *The Eleventh International Conference on Learning Representations*, 2023.

[24] Jaeho Lee and Maxim Raginsky. Minimax statistical learning with wasserstein distances. *Advances in Neural Information Processing Systems*, 31, 2018.

[25] Zijian Liu, Qinxun Bai, Jose Blanchet, Perry Dong, Wei Xu, Zhengqing Zhou, and Zhengyuan Zhou. Distributionally robust q -learning. In *International Conference on Machine Learning*, pages 13623–13643. PMLR, 2022.

[26] Carl D Meyer. *Matrix analysis and applied linear algebra*. SIAM, 2023.

[27] Mazda Moayeri, Kiarash Banihashem, and Soheil Feizi. Explicit tradeoffs between adversarial and natural distributional robustness. *Advances in Neural Information Processing Systems*, 35:38761–38774, 2022.

[28] Peyman Mohajerin Esfahani and Daniel Kuhn. Data-driven distributionally robust optimization using the wasserstein metric: performance guarantees and tractable reformulations. *Mathematical Programming*, 171(1):115–166, 2018.

[29] Hamed Rahimian and Sanjay Mehrotra. Frameworks and results in distributionally robust optimization. *Open Journal of Mathematical Optimization*, 3:1–85, 2022.

[30] Tuhin Sarkar and Alexander Rakhlin. Near optimal finite time identification of arbitrary linear dynamical systems. In Kamalika Chaudhuri and Ruslan Salakhutdinov, editors, *Proceedings of the 36th International Conference on Machine Learning*, volume 97 of *Proceedings of Machine Learning Research*, pages 5610–5618. PMLR, 09–15 Jun 2019.

[31] Renato Cesar Sato and Désirée Moraes Zouain. Markov models in health care. *Einstein (São Paulo)*, 8:376–379, 2010.

[32] Laixi Shi, Gen Li, Yuting Wei, Yuxin Chen, Matthieu Geist, and Yuejie Chi. The curious price of distributional robustness in reinforcement learning with a generative model. *Advances in Neural Information Processing Systems*, 36, 2024.

[33] Aman Sinha, Hongseok Namkoong, and John Duchi. Certifying some distributional robustness with principled adversarial training. In *International Conference on Learning Representations*, 2018.

[34] Matthew Staib, Bryan Wilder, and Stefanie Jegelka. Distributionally robust submodular maximization. In *The 22nd International Conference on Artificial Intelligence and Statistics*, pages 506–516. PMLR, 2019.

[35] Hemant Tyagi and Denis Efimov. Learning linear dynamical systems under convex constraints. *arXiv preprint arXiv:2303.15121*, 2023.

[36] Ryan Williams. Matrix-vector multiplication in sub-quadratic time:(some preprocessing required). In *SODA*, volume 7, pages 995–1001, 2007.

- [37] Virginia Vassilevska Williams, Yinzhan Xu, Zixuan Xu, and Renfei Zhou. New bounds for matrix multiplication: from alpha to omega. In *Proceedings of the 2024 Annual ACM-SIAM Symposium on Discrete Algorithms (SODA)*, pages 3792–3835. SIAM, 2024.
- [38] Huan Xu, Constantine Caramanis, and Shie Mannor. A distributional interpretation of robust optimization. *Mathematics of Operations Research*, 37(1):95–110, 2012.
- [39] Reza Yaesoubi and Ted Cohen. Generalized markov models of infectious disease spread: A novel framework for developing dynamic health policies. *European journal of operational research*, 215(3):679–687, 2011.
- [40] Shuang-Hong Yang, Bo Long, Alex Smola, Narayanan Sadagopan, Zhaojun Zheng, and Hongyuan Zha. Like like alike: joint friendship and interest propagation in social networks. In *Proceedings of the 20th international conference on World wide web*, pages 537–546, 2011.
- [41] Zhengfei Zhang, Kishan Panaganti, Laixi Shi, Yanan Sui, Adam Wierman, and Yisong Yue. Distributionally robust constrained reinforcement learning under strong duality. In *Reinforcement Learning Conference*, 2024.

A Missing and Full Proofs

A.1 Proof of Theorem 3.1

Proof. For property 1: recall that $BA = \begin{bmatrix} I_{n-1} & \mathbf{0} \\ -\mathbf{1}^\top & 0 \end{bmatrix}$. So let $M = \begin{bmatrix} \tilde{M} & \mathbf{v} \\ \mathbf{u}^\top & c \end{bmatrix}$ where $\tilde{M} \in \mathbb{R}^{(n-1) \times (n-1)}$, $\mathbf{u}, \mathbf{v} \in \mathbb{R}^{n-1}$. Note that since the matrix M is column stochastic (column sums to 1) thus $\sum_i \tilde{M}_{ij} + u_j = 1$ and $\sum_i \mathbf{v}_i + c = 1$, and thus $-\mathbf{1}^\top \tilde{M} = (\mathbf{u} - \mathbf{1})^\top$ and $-\mathbf{1}^\top \mathbf{v} = c - 1$. Then $BAM = \begin{bmatrix} \tilde{M} & \mathbf{v} \\ (\mathbf{u} - \mathbf{1})^\top & c - 1 \end{bmatrix} = M - \begin{bmatrix} \mathbf{0}^{n-1 \times n} \\ \mathbf{1}^\top \end{bmatrix}$. But each column of B is orthogonal to $\mathbf{1}$ so $B\bar{M} = BAM = MB - \mathbf{0}$. In particular, for any $\mathbf{y} \in \mathbb{R}^{n-1}$, we have $B\bar{M}\mathbf{y} = MB\mathbf{y}$, which proves that the following diagram commutes.

$$\begin{array}{ccc} \mathbb{R}^{n-1} & \xrightarrow{B} & H_n \\ \bar{M} \downarrow & & \downarrow M \\ \mathbb{R}^{n-1} & \xrightarrow{B} & H_n \end{array} \quad (4)$$

For property 2: recall that $BA = \begin{bmatrix} I_{n-1} & \mathbf{0} \\ -\mathbf{1}^\top & 0 \end{bmatrix}$. So let $M = \begin{bmatrix} \tilde{M} & \mathbf{v} \\ \mathbf{u}^\top & c \end{bmatrix}$ where $\tilde{M} \in \mathbb{R}^{(n-1) \times (n-1)}$, $\mathbf{u}, \mathbf{v} \in \mathbb{R}^{n-1}$. $MBA = \begin{bmatrix} \tilde{M} - \mathbf{v}\mathbf{1}^\top & \mathbf{0} \\ (\mathbf{u} - c\mathbf{1})^\top & 0 \end{bmatrix} = M - \begin{bmatrix} \mathbf{v}\mathbf{1}^\top & \mathbf{v} \\ c\mathbf{1}^\top & c \end{bmatrix}$. Then, $AMBA = AM - A \begin{bmatrix} \mathbf{v} \\ c \end{bmatrix} \mathbf{1}^\top$ where the all ones vector used here is of dimension n . Consider any $\mathbf{z} \in H_n$. Then, $AMBA\mathbf{z} = AM\mathbf{z} - A \begin{bmatrix} \mathbf{v} \\ c \end{bmatrix} \mathbf{1}^\top \mathbf{z}$. Since $\mathbf{z} \in H_n$, then $\mathbf{1}^\top \mathbf{z} = 0$. Hence, $AMBA\mathbf{z} = \bar{M}A\mathbf{z} = AM\mathbf{z}$ for any $\mathbf{z} \in H_n$

$$\begin{array}{ccc} \mathbb{R}^{n-1} & \xleftarrow{A} & H_n \\ \bar{M} \downarrow & & \downarrow M \\ \mathbb{R}^{n-1} & \xleftarrow{A} & H_n \end{array} \quad (5)$$

For property 3: Using $B\bar{M} = MB$ from property 1, multiply both sides by \bar{M} to obtain $B\bar{M}^2 = M\bar{M} = MMB = M^2B$. Repeating this, it follows that $B\bar{M}^t = M^tB$. Then, as $AB = I_{n-1}$ hence $AM^tB = \bar{M}^t$.

Alternately, here's a pictorial proof : take any $\mathbf{y} \in \mathbb{R}^{n-1}$ and note that by definition of B , we have $B\mathbf{y} \in H_n$. Obtain $\mathbf{x} = B\mathbf{y} + \boldsymbol{\pi}$ so that $\mathbf{x} \in \bar{\Delta}_{n-1}$ and $\mathbf{x} - \boldsymbol{\pi} \in H_n$. Then, $M\mathbf{x} = MBy + \boldsymbol{\pi}$ since $M\boldsymbol{\pi} = \boldsymbol{\pi}$. Next, $A(M\mathbf{x} - \boldsymbol{\pi}) = AMBy = \bar{M}\mathbf{y}$. These equations can be represented by the following commutative diagram.

$$\begin{array}{ccc} \mathbb{R}^{n-1} & \xrightarrow{B} & H_n \\ \bar{M} \downarrow & & \downarrow M \\ \mathbb{R}^{n-1} & \xleftarrow{A} & H_n \end{array} \quad (6)$$

By stacking $t - 1$ copies of (4) and one copy of (6) we obtain the desired property 3.

$$\begin{array}{ccc}
\mathbb{R}^{n-1} & \xrightarrow{B} & H_n \\
\overline{M} \downarrow & & \downarrow M \\
\mathbb{R}^{n-1} & \xrightarrow{B} & H_n \\
\overline{M} \downarrow & & \downarrow M \\
& \vdots & \vdots \\
\overline{M} \downarrow & & \downarrow M \\
\mathbb{R}^{n-1} & \xrightarrow{B} & H_n \\
\overline{M} \downarrow & & \downarrow M \\
\mathbb{R}^{n-1} & \xleftarrow{A} & H_n
\end{array}$$

■

A.2 Proof of Corollary 3.2

Proof. Observe that $\mathbf{x}_i - \boldsymbol{\pi} \in H_{n-1}$ (i.e., the vector components sum to 0). Thus, by second property of the theorem, $\overline{M}\mathbf{v}_i = \overline{M}A(\mathbf{x}_i - \boldsymbol{\pi}) = AM(\mathbf{x}_i - \boldsymbol{\pi}) = A(\mathbf{x}_{i+1} - \boldsymbol{\pi}) = \mathbf{v}_{i+1}$. Next, $BA = \begin{bmatrix} I_{n-1} & \mathbf{0} \\ -\mathbf{1}^\top & 0 \end{bmatrix} = I_n + \begin{bmatrix} \mathbf{0}_{(n-1) \times n} \\ -\mathbf{1}^\top \end{bmatrix}$, we can infer that $B\mathbf{v}_i = BA(\mathbf{x}_i - \boldsymbol{\pi}) = \mathbf{x}_i - \boldsymbol{\pi} + \begin{bmatrix} \mathbf{0}_{(n-1) \times n} \\ -\mathbf{1}^\top \end{bmatrix}(\mathbf{x}_i - \boldsymbol{\pi}) = \mathbf{x}_i - \boldsymbol{\pi} + \mathbf{0}$. ■

A.3 Proof of Theorem 3.3

Proof. First, we show that \overline{M} is Lyapunov stable at $\mathbf{0}$. Note if $\mathbf{x} \in \mathbb{R}^{n-1}$ then $\|\overline{M}^t \mathbf{x}\|_1 = \|AM^t B\mathbf{x}\|_1 \leq \|A\|_1 \|M\|_1^t \|B\|_1 \|\mathbf{x}\|_1 = \|A\|_1 \|B\|_1 \|\mathbf{x}\|_1$. For any given $\varepsilon > 0$ take $\delta := \frac{\varepsilon}{\|A\|_1 \|B\|_1}$. So if $\|\mathbf{x}\|_1 < \delta$ then $\|\overline{M}^t \mathbf{x}\|_1 < \|A\|_1 \|B\|_1 \delta = \varepsilon$. Then, $\|AM^t B\mathbf{y}\|_1 \leq \|A\|_1 \|M^t \mathbf{x} - \boldsymbol{\pi}\|_1 \xrightarrow{t \rightarrow \infty} 0$. Therefore \overline{M} has all eigenvalues with magnitude < 1. ■

A.4 Proof of Proposition 4.1

Proof. The following directly follow from the definitions of \mathbf{x}_t and \mathcal{U} .

$$\begin{aligned}
& \max_{\mathbf{x}_0 \in \mathcal{U}, \mathbf{q} \in \mathcal{P}} \sum_{t \in \mathcal{T}} q_t \langle \mathbf{c}, \mathbf{x}_t \rangle \\
&= \max_{\mathbf{x}_0 \in \mathcal{U}, \mathbf{q} \in \mathcal{P}} \sum_{t \in \mathcal{T}} q_t \langle \mathbf{c}, M^t \mathbf{x}_0 \rangle \\
&= \max_{\alpha_i, \mathbf{q} \in \mathcal{P}} \sum_{t \in \mathcal{T}} q_t \left(\langle \mathbf{c}, M^t \hat{\mathbf{x}}_0 \rangle + \sum_{i=1}^U \alpha_i \langle \mathbf{c}, M^t \mathbf{u}_i \rangle \right)
\end{aligned}$$

Next, let \mathbf{q}^* and α_i^* be a solution of the optimization in the last line above. Then, observe that

$$\begin{aligned}
& \sum_{t \in \mathcal{T}} q_t^* \left(\langle \mathbf{c}, M^t \hat{\mathbf{x}}_0 \rangle + \sum_{i=1}^U \alpha_i^* \langle \mathbf{c}, M^t \mathbf{u}_i \rangle \right) \\
&= \sum_{t \in \mathcal{T}} q_t^* \langle \mathbf{c}, M^t \hat{\mathbf{x}}_0 \rangle + \sum_{i=1}^U \alpha_i^* \sum_{t \in \mathcal{T}} q_t^* \langle \mathbf{c}, M^t \mathbf{u}_i \rangle
\end{aligned}$$

Let $J = \operatorname{argmax}_i \sum_{t \in \mathcal{T}} q_t^* \langle \mathbf{c}, M^t \mathbf{u}_i \rangle$. It is straightforward to check that $\alpha_i^* = 0$ for $i \notin J$. In fact, any α values with $\alpha_i = 1$ for any $i \in J$ is a feasible solution that yields the same optimal solution value. Thus, there exists an optimal solution that has $\alpha_i = 1$ and vertex u_i selected. This leads to the simple algorithm enumerated below

1. Iterate over all vertices u_i and solve $\max_{\mathbf{q} \in \mathcal{P}} \sum_{t \in \mathcal{T}} q_t \langle \mathbf{c}, M^t (\hat{\mathbf{x}}_0 + u_i) \rangle$
2. Choose the best solution value from the above loop.

This algorithm is exactly same as $\max_{i \in [U]} \max_{\mathbf{q} \in \mathcal{P}} \sum_{t \in \mathcal{T}} q_t \langle \mathbf{c}, M^t (\hat{\mathbf{x}}_0 + \mathbf{u}_i) \rangle$ ■

A.5 Proof of Lemma 5.1

Proof. The complexity of finding M^B is $\mathcal{O}(n^\omega \log B)$ as there are about $\log B$ squares and multiplications in the successive squaring (matrix products). Complexity of precomputing B such terms is $\mathcal{O}(n^{2+\varepsilon} + Bn^2/(\varepsilon \log n)^2)$. Similarly, for precomputing the matrix transpose powers we get $\mathcal{O}(n^{2+\varepsilon} + Bn^2/(\varepsilon \log n)^2)$. The first for loop has time complexity of $\mathcal{O}(nT)$ because of one dot product in the loop that runs B^2 times. The second loop does a matrix-vector product with the same matrix M a max of \sqrt{T} times, which has time complexity $\mathcal{O}\left(n^{2+\varepsilon} + \sqrt{T}n^2/(\varepsilon \log n)^2\right)$ ■

A.6 Proof of Proposition 5.2

Proof. Let's write $\|\cdot\|$ for $\|\cdot\|_W^d$. Call $C := \{\mathbf{x} \in \mathbb{R}^T \mid |x_i - x_j| \leq d_{ij} \forall i, j\}$. Note that $\mathbf{x} \in C \iff -\mathbf{x} \in C$.

- (Homogeneity) If $\boldsymbol{\mu} \in H_T, \lambda \in \mathbb{R}$ then $\|\lambda \boldsymbol{\mu}\| = \max_{\mathbf{x} \in C} \lambda \boldsymbol{\mu}^\top \mathbf{x} = |\lambda| \max_{\mathbf{x} \in C} \boldsymbol{\mu}^\top \mathbf{x} = |\lambda| \|\boldsymbol{\mu}\|$ because \mathbf{x} can be replaced with $-\mathbf{x}$ depending on the sign of λ .
- (Positive definiteness) Since $\mathbf{x} \in C \iff -\mathbf{x} \in C$, we see that $\|\boldsymbol{\mu}\| \geq 0$ always. Suppose $\|\boldsymbol{\mu}\| = 0$ for some $\boldsymbol{\mu} \in G_T$. Then $\boldsymbol{\mu} \leq 0 \forall \mathbf{x} \in C$ by definition. Let $\alpha_i := \min_{j \in [T] \setminus \{i\}} d_{ij}$. Clearly each $\alpha_i > 0$ and each $\boldsymbol{\omega}_i := \alpha_i \mathbf{e}_i \in C$. The latter is true because for $k \neq j, j \neq i$ $|(\boldsymbol{\omega}_i)_k - (\boldsymbol{\omega}_i)_j| = \begin{cases} \alpha_i & \text{if } k = i \\ 0 & \text{otherwise} \end{cases} \leq d_{kj}$. It follows that $0 \geq \boldsymbol{\mu}^\top \boldsymbol{\omega}_i = \alpha_i \mu_i$. But $\alpha_i > 0$ whence $\mu_i \leq 0 \forall i$. The only $\boldsymbol{\mu} \in H_T$ with all non-positive coordinates is $\boldsymbol{\mu} = \mathbf{0}$.
- (Triangle inequality) Take any $\boldsymbol{\mu}, \boldsymbol{\nu} \in H_T$. Then for each $\mathbf{x} \in C$ we have $(\boldsymbol{\mu} + \boldsymbol{\nu})^\top \mathbf{x} = \boldsymbol{\mu}^\top \mathbf{x} + \boldsymbol{\nu}^\top \mathbf{x} \leq \max_{\mathbf{y} \in C} \boldsymbol{\mu}^\top \mathbf{y} + \max_{\mathbf{z} \in C} \boldsymbol{\nu}^\top \mathbf{z} = \|\boldsymbol{\mu}\| + \|\boldsymbol{\nu}\|$. It thus stands that $(\boldsymbol{\mu} + \boldsymbol{\nu})^\top \mathbf{x} \leq \|\boldsymbol{\mu}\| + \|\boldsymbol{\nu}\| \forall \mathbf{x} \in C$. Taking max over $\mathbf{x} \in C$ gives $\|\boldsymbol{\mu} + \boldsymbol{\nu}\| \leq \|\boldsymbol{\mu}\| + \|\boldsymbol{\nu}\|$. ■

A.7 Proof of Theorem 5.3

Proof. First, recall the standard known Farkas lemma.

Lemma A.1 (Farkas lemma). *Let $B \in \mathbb{R}^{d \times e}, \mathbf{b} \in \mathbb{R}^d$ then exactly one of the following sets is empty:*

- (a) $\{\mathbf{x} \in \mathbb{R}^e \mid B\mathbf{x} = \mathbf{b}, \mathbf{x} \geq 0\}$.
- (b) $\{\mathbf{y} \in \mathbb{R}^d \mid B^\top \mathbf{y} \leq 0, \mathbf{b}^\top \mathbf{y} > 0\}$.

For the Wasserstein ball of radius 1 around $\mathbf{0} \in \mathbb{R}^T$, we want to find those $\boldsymbol{\mu} \in H_T$ such that $\boldsymbol{\mu}^\top \mathbf{x} \leq 1$ for every $\mathbf{x} \in H_T$ satisfying $A\mathbf{x} \leq \mathbf{1}, \mathbf{1}^\top \mathbf{x} \leq 0, -\mathbf{1}^\top \mathbf{x} \leq 0$. Here A is the matrix whose rows comprise of the constraint vectors $\frac{\mathbf{e}_i - \mathbf{e}_j}{d_{ij}}$, hence A has $m = T(T-1)$ rows. Also, $\mathbf{1}^\top \mathbf{x} \leq 0, -\mathbf{1}^\top \mathbf{x} \leq 0$ is same as $\mathbf{1}^\top \mathbf{x} = 0$, which enforces $\mathbf{x} \in H_T$.

Take $W = \begin{bmatrix} A \\ \mathbf{1}^\top \\ -\mathbf{1}^\top \end{bmatrix} \in \mathbb{R}^{(m+2) \times T}$ and $\mathbf{v} = \begin{bmatrix} \mathbf{1} \\ 0 \\ 0 \end{bmatrix} \in \mathbb{R}^{m+2}$. Then, $A\mathbf{x} \leq \mathbf{1}, \mathbf{1}^\top \mathbf{x} \leq 0, -\mathbf{1}^\top \mathbf{x} \leq 0$ can be written as $W\mathbf{x} \leq \mathbf{v}$.

Fix such a $\boldsymbol{\mu}$ in the Wasserstein unit ball around $\mathbf{0}$. Then $S := \{\mathbf{x} \in \mathbb{R}^T \mid W\mathbf{x} \leq \mathbf{v}, \boldsymbol{\mu}^\top \mathbf{x} - 1 > 0\}$ must be empty. We have an alternate representation as $S = \left\{ \mathbf{x} \in \mathbb{R}^T \mid [W \ -\mathbf{v}] \begin{bmatrix} \mathbf{x} \\ 1 \end{bmatrix} \leq \mathbf{0}, [\boldsymbol{\mu}^\top \ -1] \begin{bmatrix} \mathbf{x} \\ 1 \end{bmatrix} > 0 \right\}$. Define $B := \begin{bmatrix} W^\top \\ -\mathbf{v}^\top \end{bmatrix}, \mathbf{b} := \begin{bmatrix} \boldsymbol{\mu} \\ -1 \end{bmatrix}$. Now homogenize S to $S' := \{\mathbf{u} \in \mathbb{R}^{T+1} \mid B^\top \mathbf{u} \leq \mathbf{0}, \mathbf{b}^\top \mathbf{u} > 0\}$. Note that the last component of vector \mathbf{u} in S' is a free variable as opposed to the last component in S . So while S is empty, we need a proof for the claim below:

Claim. $S' = \emptyset$.

Proof. We always denote $\mathbf{u} = \begin{bmatrix} \mathbf{x} \\ y \end{bmatrix}$ with $\mathbf{x} \in \mathbb{R}^T, y \in \mathbb{R}$. Recall that $B^\top = [W \ -\mathbf{v}] = \begin{bmatrix} A & -\mathbf{1} \\ \mathbf{1}^\top & 0 \\ -\mathbf{1}^\top & 0 \end{bmatrix}$. Suppose $\mathbf{u} \in S'$. Then the first m rows of $B^\top \mathbf{u} \leq \mathbf{0}$ gives the condition that $A\mathbf{x} \leq y$, i.e., $x_i - x_j \leq y \forall i \neq j$. Adding the inequalities for, say $(i, j) = (1, 2), (2, 1)$, gives $y \geq 0$. Consider the following two cases.

$y = 0$: The first m rows give the condition $x_i - x_j \leq 0 \forall i \neq j$ and the last two rows give that $\mathbf{1}^\top \mathbf{x} = 0$. The former implies $x_i = x_j \forall i \neq j$. Combined with $\mathbf{1}^\top \mathbf{x} = 0$, we get $\mathbf{x} = \mathbf{0}$. So $\mathbf{u} = 0$ is the only candidate with last coordinate 0 that satisfies $B^\top \mathbf{u} \leq \mathbf{0}$. But this does not satisfy $\mathbf{b}^\top \mathbf{u} > 0$. So S' has no element with last coordinate 0.

$y > 0$: Then the vector $\mathbf{v} = \frac{1}{y} \mathbf{u} = \begin{bmatrix} \frac{1}{y} \mathbf{x} \\ 1 \end{bmatrix} \in S = \emptyset$. This is impossible. ■

Then, $\left\{ \boldsymbol{\alpha} = \begin{bmatrix} \boldsymbol{\lambda} \\ r \\ s \end{bmatrix} \in \mathbb{R}^{m+2} \mid B\boldsymbol{\alpha} = \mathbf{b}, \boldsymbol{\alpha} \geq 0 \right\} \neq \emptyset$ by Farkas Lemma A.1. Pick one such element $\begin{bmatrix} \boldsymbol{\lambda} \\ r \\ s \end{bmatrix}$ of this set. Recall $B = \begin{bmatrix} A^\top & \mathbf{1} & -\mathbf{1} \\ -\mathbf{1}^\top & 0 & 0 \end{bmatrix} \in \mathbb{R}^{(T+1) \times (m+2)}, \mathbf{b} = \begin{bmatrix} \boldsymbol{\mu} \\ -1 \end{bmatrix} \in \mathbb{R}^{T+1}$. The last row constraint gives $-\mathbf{1}^\top \boldsymbol{\lambda} = -1$ so that $\mathbf{1}^\top \boldsymbol{\lambda} = 1$. The first T row constraints give $A^\top \boldsymbol{\lambda} + (r - s)\mathbf{1} = \boldsymbol{\mu}$. But $\boldsymbol{\mu} \in H_T$. So $\mathbf{1}^\top \boldsymbol{\mu} = 0 \implies (A\mathbf{1})^\top + (r - s)\mathbf{1}^\top \mathbf{1} = (r - s)T \implies r = s \implies \boldsymbol{\mu} = A^\top \boldsymbol{\lambda}$. Here we used the fact that $A\mathbf{1} = \mathbf{0}_m$ because each row of A sums to 0. A typical column of A^\top looks like $\mathbf{v}_{ij} = \frac{\mathbf{e}_i - \mathbf{e}_j}{d_{ij}}$. This establishes that $\exists \boldsymbol{\lambda} \in (\mathbb{R}_{\geq 0})^m$ indexed by $(i, j), i \neq j$, such that $\sum_{j \neq i} \lambda_{ij} = 1$ and $\boldsymbol{\mu} = \sum_{j \neq i} \lambda_{ij} \mathbf{v}_{ij}$. It can be easily checked that the \mathbf{v}_{ij} 's satisfy our required criterion of the Wasserstein distance from $\mathbf{0}$ being 1. ■

A.8 Proof of Proposition 5.4

Proof. $\zeta = \max \{|\lambda_p|, r_q\} < 1$. For $t > n_0$ we have $\zeta^t < \frac{g(t_0)}{\sum |d_i| + \sum |w_j|}$ whence $|g(t)| \leq \sum |d_i| r_i^t + \sum |w_j \lambda_j^t| \leq \left(\sum |d_i| + \sum |w_j| \right) \zeta^{t'} < g(t_0)$. ■

A.9 Proof of Proposition 5.5

Proof. We already know $\left| \frac{g(t)}{|\lambda_p|^t} - w_p (\operatorname{sgn} \lambda_p)^t \right| = \left| \sum_{i=1}^q \frac{d_i r_i^t}{|\lambda_p|^t} + \sum_{j=1}^{p-1} \frac{w_j \lambda_j^t}{|\lambda_p|^t} \right| \leq \sum_{i=1}^q |d_i| \left| \frac{r_i^t}{\lambda_p^t} \right| + \sum_{j=1}^{p-1} |w_j| \left| \frac{\lambda_j^t}{\lambda_p^t} \right| \leq \left(\sum_{i=1}^q |d_i| + \sum_{j=1}^{p-1} |w_j| \right) \varepsilon^t = \beta \varepsilon^t$. ■

A.10 Proof of Lemma 5.6

Proof. We prove each bullet point respectively as follows.

- $w_p > 0, \lambda_p > 0$:
 $t_0 > \log_\varepsilon \left(\frac{w_p}{\beta} \right) \implies \varepsilon^{t_0} < \frac{w_p}{\beta}$. The last implication is because $\varepsilon < 1$. Since $w_p, \lambda_p > 0$, Proposition 5.5 gives $\left| \frac{g(t_0)}{|\lambda_p|^{t_0}} - w_p \right| < w_p$. This means $\frac{g(t_0)}{|\lambda_p|^{t_0}} > 0$ whence $g(t_0) > 0$.
- $w_p > 0, \lambda_p < 0$:
We use a similar reasoning as above. If t_0 is even and $\frac{t_0}{2} > \frac{1}{2} \log_\varepsilon \left(\frac{w_p}{\beta} \right)$, that is, $t_0 > \log_\varepsilon \left(\frac{w_p}{\beta} \right)$ then Proposition 5.5 gives us $\left| \frac{g(t_0)}{|\lambda_p|^{t_0}} - w_p \right| \leq \beta \varepsilon^{t_0} < w_p$ which again implies that $g(t_0) > 0$.
- $w_p < 0, \lambda_p < 0$:
Again, use similar reasoning as the first bullet point. t_0 being odd here ensures that $w_p (\operatorname{sgn} \lambda_p)^{t_0} = -w_p > 0$. Here we again have $t_0 > \log_\varepsilon \left(\frac{-w_p}{\beta} \right)$. Proposition 5.5 turns into $\left| \frac{g(t_0)}{|\lambda_p|^{t_0}} + w_p \right| < -w_p$ whence $g(t_0) > 0$.

For the final case when $w_p < 0, \lambda_p > 0$, if $t > \log_\varepsilon \left(\frac{-w_p}{\beta} \right)$ then $\varepsilon^t < \frac{-w_p}{\beta}$ as earlier. For such $t \in \mathbb{N}$, Proposition 5.5 gives $\left| \frac{g(t)}{|\lambda_p|^t} - w_p \right| \leq \beta \varepsilon^t < -w_p$ whence $g(t) < 0$. So if $g(t) < 0$ for each $t \leq t_0 := \left\lfloor \log_\varepsilon \left(\frac{-w_p}{\beta} \right) \right\rfloor$ then g is always negative on \mathbb{N} . ■

A.11 Proof of Proposition 5.7

Proof. We already know $\left| \frac{g(t)}{r_q^t} - d_q \cos(t\theta_q + \eta_q) \right| = \left| \sum_{i=1}^{q-1} \frac{d_i r_i^t}{r_q^t} + \sum_{j=1}^p \frac{w_j \lambda_j^t}{r_q^t} \right| \leq \sum_{i=1}^{q-1} |d_i| \left| \frac{r_i^t}{r_q^t} \right| + \sum_{j=1}^p |w_j| \left| \frac{\lambda_j^t}{r_q^t} \right| \leq \left(\sum_{i=1}^{q-1} |d_i| + \sum_{j=1}^p |w_j| \right) C^t = \gamma C^t$. ■

A.12 Proof of Lemma 5.8

Proof. We first want to show that $\exists k \in \mathbb{Z}_{>0}$ s.t. $\cos(k\theta_q + \eta_q) \geq 0.5$ and $k' \in \mathbb{Z}_{>0} \cos(k'\theta_q + \eta_q) \leq -0.5$, which can be found in $\mathcal{O}(\log(\min(a, b)))$.

Write θ, η, d for θ_q, η_q, d_q respectively. Let's first do the calculation assuming $d > 0$. Let ε be such that $\arccos \varepsilon = 50$. If we find some integers $k > 0, m$ such that $k\theta + \eta \in (360m - 50, 360m + 50)$, this implies that $\cos(k\theta + \eta) > \varepsilon > 0.5$. Next,

$$k\theta + \eta \in (360m - 50, 360m + 50) \implies k\theta \in (360m - 50 - \eta, 360m + 50 - \eta)$$

Then, we need to find $k > 0, m$ such that $k\theta \in (360m - 50 - \eta, 360m + 50 - \eta)$.

Consider $i = \lfloor \eta \rfloor$. It is enough to find k such that (note inclusive below)

$$k\theta \in [360m - 45 - i, 360m + 45 - i]$$

The above is equivalent to $k\theta + 45 + i - 360m \in [0, 90]$.

Let us use a shortform $c = 45 + i$. Let $\theta = a/b$ and $0 \leq z \leq 90$. Choose $z = p/b$, for any $0 < p < 90b$. Then, we want to show that $k\theta + c = 360m + z$ for some positive integer k and an integer m .

From now on we treat k, m as integer variables which we solve for. Substituting the fractions, we need to solve $k \cdot a - m \cdot 360b = p - cb$. Since $\gcd(a, b) = 1$ so $\gcd(a, 360b) = \gcd(a, 360) = g$. Then, a/g and $360b/g$ are relatively prime, and $g \mid p - cb$ (read \mid as divides). By Bezout's identity, there are integers n, l such that $n \cdot a/g + l \cdot 360b/g = 1$. We claim that $n \neq 0$ because if it were, then $l = 360b/g = 1$ so that $g \mid 360$ (as $\gcd(g, b) \leq \gcd(a, b) = 1$), which would mean that $g = 360$ further implying $a \geq 360$ and $b = 1$ making $\theta \geq 360$ but we had assumed $\theta < 360$.

Say $n > 0$: Choose integer $s \geq 0$ such that $\alpha_s := (p - cb)/g + s \cdot 360b/g > 0$. Then $n\alpha_s \cdot a/g + l\alpha_s \cdot 360b/g = \alpha_s$.

Say $n < 0$: Choose integer $s \leq 0$ such that $\alpha_s := (p - cb)/g + s \cdot 360b/g < 0$. Then $n\alpha_s \cdot a/g + l\alpha_s \cdot 360b/g = \alpha_s$.

Combined we can say that with $s_0 := 1 + \max \left\{ 0, \left\lceil \frac{\operatorname{sgn}(n)(cb - p)}{360} \right\rceil \right\}$ and $f \geq 0$ we have that $\alpha = \alpha_{\operatorname{sgn}(n)(s_0 + f)}$ satisfies $n\alpha \cdot a/g + l\alpha \cdot 360b/g = \alpha$ with $n\alpha > 0$. Thus we have found infinitely many solutions for (k, m) , namely $\{(n\alpha_{\operatorname{sgn}(n)(s_0 + f)}, s_0 + \operatorname{sgn}(n)t - l\alpha_{\operatorname{sgn}(n)(s_0 + f)}) \mid f \in \mathbb{Z}, f \geq 0\}$. The important point is that each aforementioned solution for k , that is $n\alpha_{\operatorname{sgn}(n)(s_0 + f)}$, is positive and is a strictly increasing sequence. In fact, the expression equals $n\alpha_{\operatorname{sgn}(n)(s_0 + f)} = n(p - cb)/g + |n|(s_0 + f)360b/g$ for $f \geq 0$ and is always positive. Define $k_f := n(p - cb)/g + |n|(s_0 + f)360b/g$. They satisfy that $\cos(k_f\theta + \eta) \geq 0.5$ whence by Proposition 5.7, we conclude that for any positive integer $f \geq \frac{g \log_C(\frac{d}{2\gamma}) - n(p - cb)}{360b|n|} - s_0$, we have $g(k_f) > 0$ because such a choice of f makes $\gamma C^{k_f} < \frac{d}{2}$.

If $d < 0$ we seek to solve the same problem but with $\cos(k\theta + \eta) < -0.5$ and this is equivalent to $\cos(k\theta + 180 + \eta) > 0.5$. That is, we can repeat the above steps by replacing η with $\eta + 180$. So we want to find t for which $\gamma C^t < \frac{-d}{2}$ and this is achieved with $k_f = n(p - c'b)/g + |n|(s'_0 + f)360b/g$ where $c' = 45 + i + 180$ and s'_0 is the same expression as s_0 above, but c replaced with c' .

Putting these together, our t_0 takes the form

$$\frac{n(p - bc) + |n| \left(s_0 + \max \left\{ 1, \left\lceil \frac{g \log_C(\frac{|d|}{2\gamma}) - n(p - cb)}{360b|n|} - s_0 \right\rceil \right\} \right) 360b}{g}$$

where $s_0 = 1 + \max \left\{ 0, \left\lceil \frac{\operatorname{sgn}(n)(cb - p)}{360} \right\rceil \right\}$ and $c = 135 + i - \operatorname{sgn}(d) \cdot 90$.

In the above solving for the n, l using Bezout's identity can be done by Extended Euclid's algorithm, which takes time of the order of the smaller of bit representation of a/g and $360b/g$. And with a worst case of $g = 1$, this is $\mathcal{O}(\log(\min(a, b)))$, which is the dominating computation. \blacksquare

A.13 Proof of Theorem 5.9

Proof. The following decision problem is known to be NP-hard [4]: (DIRCYC) Given a directed graph G on n nodes, is there an integer $t^* \in \mathbb{N}$ such that G has no directed path of length t^* from node 1 to node n ?

We will show a reduction from this problem to the problem of our interest. Let $n \in \mathbb{N}$ and graph G be an input to DIRCYC. We describe an input to our problem as follows. Let A be the adjacency matrix of G . It is well known that $p_i^{(j)} := \mathbf{e}_1^\top A^j \mathbf{e}_i = (A^j)_{1i}$ is the number of directed walks of length j from 1 to i in G . Let $r = 1 + \max_i \sum_j A_{ij}$. Proposition C.1 (in appendix) for $p = 1$ implies $\rho(A) \leq r - 1$.

So $\frac{1}{r}A$ has all eigenvalues of size < 1 . Take inputs as $n, M = \frac{1}{r}A, \mathbf{a} = \mathbf{e}_n, \alpha = 0, \mathbf{c} = \mathbf{e}_1$. Note that for any $t \in \mathbb{N}$, $\langle \mathbf{c}, A^t \mathbf{a} \rangle = p_n^{(t)}$ for the aforementioned inputs.

We claim $\exists t^* \in \mathbb{N}$ for which G has no directed path from 1 to n of length t^* iff $\exists t^* \in \mathbb{N}$ such that $\langle \mathbf{c}, M^{t^*} \mathbf{a} \rangle \leq \alpha$. Indeed, $\exists t^* \in \mathbb{N}$ such that $\langle \mathbf{c}, M^{t^*} \mathbf{a} \rangle \leq \alpha \iff \frac{p_n^{(t^*)}}{r^{t^*}} \leq 0 \iff p_n^{(t^*)} \leq 0 \iff p_n^{(t^*)} = 0 \iff G$ has no directed path from 1 to n of length t^* . \blacksquare

A.14 Proof of Lemma 5.10

Proof. We start with an $n = 2$ proof and will extend it to general n later. Consider $\alpha_k, \theta_k \in \mathbb{Q}$ and inputs $\mathbf{c}_k, \mathbf{x}_k, M_k$ as follows: $\mathbf{c}_k = (1, 0), \mathbf{x}_k = (\cos \alpha_k, \sin \alpha_k), M_k = \frac{1}{2} \begin{bmatrix} \cos \theta_k & -\sin \theta_k \\ \sin \theta_k & \cos \theta_k \end{bmatrix}$.

The factor $\frac{1}{2}$ was used because $2M_k$ has all distinct eigenvalues of size 1, whence M_k has all eigenvalues of size < 1 . In other words, $\rho(M_k) < 1$. Thus, $2^t g(t) = 2^t \mathbf{c}_k^\top M_k^t \mathbf{x}_k = \cos \alpha_k \cos t\theta_k - \sin \alpha_k \sin t\theta_k = \cos(\alpha_k + t\theta_k)$.

We show there exist $\alpha_k, \theta_k \in \mathbb{Q}$ such that $g(t)$ is negative for any $t \in [k]$. It is well known from arctan series (Taylor expansion of \tan^{-1}) that $\frac{\pi}{4} = 1 - \frac{1}{3} + \frac{1}{5} - \frac{1}{7} + \dots$. Take $x_i := \frac{1}{2i-1}$. Then, it is also known that

$$\left| \frac{\pi}{4} - \sum_{i=1}^k (-1)^{i+1} x_i \right| \leq x_{k+1} = \frac{1}{2k+1}.$$

So $\left| \frac{\pi}{2} - \sum_{i=1}^k (-1)^{i+1} 2x_i \right| \leq 2x_{k+1} = \frac{2}{2k+1}$. Consider the terms

$$s_i := 2x_{2i-1} - 2x_{2i} = \frac{2}{4i-3} - \frac{2}{4i-1} = \frac{4}{(4i-1)(4i-3)} > 0.$$

This gives

$$\left| \frac{\pi}{2} - \sum_{i=1}^k s_i \right| = \left| \frac{\pi}{2} - \sum_{i=1}^{2k} (-1)^{i+1} 2x_i \right| \leq 2x_{2k+1} = \frac{2}{4k+1}.$$

This proves that $\lim_{k \rightarrow \infty} \sum_{i=1}^k s_i = \frac{\pi}{2}$ and the convergence is monotone. So

$$\frac{\pi}{2} - \sum_{i=1}^k s_i = \left| \frac{\pi}{2} - \sum_{i=1}^k s_i \right| \leq \frac{2}{4k+1}. \quad (7)$$

Let $\alpha_k := \sum_{i=1}^k s_i$ and $\theta_k := \frac{2}{4k+1}$. Since $\alpha_k \uparrow \pi/2$, we have $\cos \alpha_k > 0, \sin \alpha_k > 0$

- From Equation 7, $\frac{\pi}{2} < \alpha_k + \theta_k$.
- If $t > 1$ is a positive integer, then $t\theta_k + \alpha_k > \theta_k + \alpha_k$ because $\theta_k > 0$.
- Finally

$$k\theta_k = \frac{2k}{4k+1} < \frac{1}{2} < \frac{\pi}{2} < \left(\frac{\pi}{2} - \alpha_k \right) + \frac{\pi}{2} = \pi - \alpha_k \implies k\theta_k + \alpha_k < \pi.$$

The above bullet points prove that

$$\frac{\pi}{2} < \alpha_k + \theta_k < \alpha_k + 2\theta_k < \dots < \alpha_k + k\theta_k < \pi.$$

We know that \cos is strictly decreasing over $[0, \pi]$ and thus

$$0 > \cos(\alpha_k + t\theta_k) = 2^t g(t) > -1 \text{ for all integers } t \in [k].$$

We have thus shown that the first positive integer t , if any, satisfying $\cos(\alpha_k + t\theta_k) > 0$ must satisfy $t > k$. In fact, $t = 9k$ is such a candidate. Indeed,

$$\frac{5\pi}{2} > \pi + 4 > \pi + \frac{16k}{4k+1} = \pi + 8k\theta_k > \alpha_k + 9k\theta_k$$

and

$$\alpha + 9k\theta_k > \frac{\pi}{2} - \theta_k + 9k\theta_k = \frac{18k-2}{4k+1} + \frac{\pi}{2} \stackrel{[::k \geq 1]}{\geq} \frac{16}{5} + \frac{\pi}{2} > \frac{3\pi}{2}.$$

Since $\alpha_k + 9k\theta_k$ is between $\frac{3\pi}{2}, \frac{5\pi}{2}$, we must have $\cos(\alpha_k + 9k\theta_k) > 0$. This proves our desired result for $n = 2$.

Take $\tilde{M}_k = \begin{bmatrix} M_k & & & \\ & 2^{-1} & & \\ & & 3^{-1} & \\ & & & \ddots \\ & & & & (n-1)^{-1} \end{bmatrix} \in \mathbb{R}^{n \times n}$, $\tilde{\mathbf{x}}_k = (\mathbf{x}, 0, \dots, 0) \in \mathbb{R}^n$, $\tilde{\mathbf{c}}_k = \mathbf{e}_1 \in \mathbb{R}^n$, then \tilde{M}_k has all distinct eigenvalues of size < 1 and $\tilde{\mathbf{c}}_k^\top \tilde{M}_k \tilde{\mathbf{c}}_k = \mathbf{c}_k^\top M_k \mathbf{x}_k$. We thus get the same behaviour for $n \times n$ matrices. \blacksquare

A.15 Proof for Proposition 5.11

Proof. We obtain n_0 directly from application of from Proposition 5.4 by replacing $g(t_0)$ by ε . Then, the CDF for \mathbf{q}_ρ is $1 - (1 - \rho)^t$. Thus, $|\sum_{t=n_0+1}^{\infty} g(t)q_\rho(t)| \leq \varepsilon \sum_{t=n_0+1}^{\infty} q_\rho(t) = \varepsilon\delta$. \blacksquare

B Special case for $n = 2$

In this special case for the infinite support, we can provide a better bound on t_0 . Recall that if M has purely imaginary eigenvalues with the angle parameter of its Jordan form given by θ , $r = \det M > 0$, $\langle \mathbf{c}, M^t \mathbf{x} \rangle = r^t(a_1 \cos t\theta - a_2 \sin t\theta)$ where a_1, a_2 are completely determined by $\mathbf{c}, \mathbf{x}, M$. We let $d > 0, \kappa > 0, \alpha \in (0, 2\pi), \gamma \in (0, 2\pi)$ be such that $a_1 + ia_2 = de^{i\alpha}$ and $\ln r + i\theta = \kappa e^{i\gamma}$. We assume $\alpha, \theta, \gamma \in \mathbb{Q}$.

Lemma B.1. If $\theta \in (0, \pi)$ then for $t_0 := \left\lceil \frac{-\frac{\pi}{2} - \alpha + 2\pi \cdot \lceil \frac{\alpha}{2\pi} + \frac{1}{4} \rceil}{\theta} \right\rceil$ we have $g(t_0) > 0$. Consider

$\left\{ x_m := \frac{\frac{\pi}{2} - \alpha - \gamma + m\pi}{\theta} \mid m \in \mathbb{Z} \right\}$. Moreover for $m^* := 1 + \left\lceil \frac{\theta \log_r \left(\frac{g(t_0)}{|\sin \gamma| d} \right) + \alpha + \gamma - \frac{\pi}{2}}{\pi} \right\rceil$,

we have $\sup_{t \in \mathbb{N}} g(t) = \sup_{1 \leq t \leq x_{m^*}} g(t)$.

Proof. For non-real complex eigenvalues, $J = r \begin{bmatrix} \cos \theta & -\sin \theta \\ \sin \theta & \cos \theta \end{bmatrix}$. Then, $J^t = r^t \begin{bmatrix} \cos t\theta & -\sin t\theta \\ \sin t\theta & \cos t\theta \end{bmatrix}$ whence $\langle \mathbf{c}, M^t \mathbf{x} \rangle = r^t(a_1 \cos t\theta - a_2 \sin t\theta)$ where a_1, a_2 are constants completely determined by the inputs $\mathbf{c}, \mathbf{x}, M$.

Let's try to see where $r^t(a_1 \cos t\theta - a_2 \sin t\theta)$ maximizes. First extend to a real function $g(x) := r^x(a_1 \cos x\theta - a_2 \sin x\theta) = \Re(e^{ix\theta}(a_1 + ia_2))$ so that $g'(x) = r^x \Re(e^{ix\theta} \cdot (\ln r + i\theta) \cdot (a_1 + ia_2))$ where $\Re(\cdot)$ denotes the real part of complex numbers.

Let's name the above complex numbers as $u := \ln r + i\theta = \kappa e^{i\gamma}$ and $a := a_1 + ia_2 = de^{i\alpha}$ where $\kappa, d > 0$ and $\alpha, \gamma \in (0, 2\pi)$. But $r \in (0, 1), \theta \neq \pi$ means that $\gamma \in (\frac{\pi}{2}, \frac{3\pi}{2})$ and $\sin \gamma \neq \frac{\pi}{\kappa}$. With this we have $g(x) = r^x \cos(x\theta + \alpha)$. We assumed $\alpha, \theta \in \mathbb{Q}$.

Now we find all those x such that $g'(x) = 0$ and $g(x) > 0$ (such an x automatically satisfies $g''(x) \leq 0$). Let's first focus on the solutions of $g'(x) = 0$, that is, all x satisfying $\Re(e^{i(x\theta + \alpha + \gamma)}) =$

$\frac{1}{\kappa d} \Re(e^{ix\theta} ua) = 0$. The solutions are $\left\{ x_m := \frac{\frac{\pi}{2} - \alpha - \gamma + m\pi}{\theta} \mid m \in \mathbb{Z} \right\}$. They satisfy

$$g(x_m) = (-1)^m r^{x_m} d \sin \gamma.$$

Thus $\{|g(x_m)|\}_{m \geq 0}$ is a strictly decreasing sequence in terms of m . In fact, the local maxima over the positive reals are exactly the points $\{x_{2m}\}_{m \in \mathbb{N}_0}$. The issue in finding $\sup_{t \in \mathbb{N}} g(t)$ is that these x_m 's are merely real numbers.

However, if we could find some $t_0 \in \mathbb{N}$ such that $g(t_0) > 0$, taking $\varepsilon = g(t_0)$ gives an N such that $g(x_m) < \varepsilon \forall m > N$, whence the required supremum occurs only over $\mathbb{N} \cap [1, x_{N-1}]$. Now take t_0 to be as in the statement of the lemma.

For brevity let's call $p := \frac{\alpha}{2\pi} + \frac{1}{4}$ and $q := \lceil p \rceil$ (this choice of q makes $t_0 > 0$). Clearly $t_0\theta + \alpha \geq 2\pi q - \frac{\pi}{2}$. It was earlier assumed that $\alpha, \theta \in \mathbb{Q}$ so the last inequality is strict. This means that $\frac{-\frac{\pi}{2} - \alpha + 2\pi q}{\theta} \notin \mathbb{Z}$.

The following thus holds:

$$\begin{aligned} \frac{-\frac{\pi}{2} - \alpha + 2\pi q}{\theta} &< t_0 \leq \frac{-\frac{\pi}{2} - \alpha + 2\pi q}{\theta} + 1 \\ \implies 2\pi q - \frac{\pi}{2} &< t_0\theta + \alpha \leq -\frac{\pi}{2} + 2\pi q + \theta \stackrel{[\because \theta < \pi]}{<} 2\pi q + \frac{\pi}{2}. \end{aligned}$$

It thus stands that $\Re(e^{it_0\theta} \cdot a) = d \cos(t_0\theta + \alpha) > 0$ which has the same sign as $g(t_0)$.

For the latter part, notice that if $m \geq m^*$ then $x_m > \log_r \left(\frac{g(t_0)}{d|\sin \gamma|} \right)$ whence $\ln |g(x_{m^*})| \leq \ln |g(x_m)| = x_m \underbrace{\ln r}_{<0} + \ln(d|\sin \gamma|) < \log_r \left(\frac{g(t_0)}{d|\sin \gamma|} \right) \ln r + \ln(d|\sin \gamma|) = \ln(g(t_0))$. So $t > x_{m^*}$ implies that $g(t) \leq |g(x_{m^*})| < g(t_0)$. The first inequality here is because if $x \geq x_k$ is a real number then $|g(x)| = r^x |\cos(x\theta + \alpha)| \leq r^x \leq r^{x_k} \leq r^{x_k} \cdot 1 = r^{x_k} \cdot |\cos(x_k\theta + \alpha)| = |g(x_k)|$. \blacksquare

C Miscellaneous Results and Clarifications

Proposition C.1. $\rho(A) \leq \|A\|_p$ for any $p \in \mathbb{R}_{\geq 1}$ for any $A \in \mathbb{C}^{n \times n}$.

Proof. If $\lambda \in \mathbb{C}$ is an eigenvalue of A such that $\rho(A) = |\lambda|$ then $\exists \mathbf{u} \in \mathbb{C}^n$ such that $\|\mathbf{u}\|_p = 1$ and $A\mathbf{u} = \lambda\mathbf{u}$ whence $\|A\|_p \geq \|A\mathbf{u}\|_p = \|\lambda\mathbf{u}\|_p = |\lambda| = \rho(A)$. \blacksquare

All different eigenvalues assumption: Note that for a GAS system the highest magnitude eigenvalue determines the rate of convergence to $\mathbf{0}$. Thus, if there are two eigenvalues exactly same with the highest magnitude, perturbing one of them so that magnitude reduces by ε for arbitrarily small ε does not affect the convergence to $\mathbf{0}$ or the rate of convergence. The other non-highest magnitude eigenvalues can also be perturbed similarly with no effect on the convergence to $\mathbf{0}$ or the rate of convergence.

Another plausible approach instead of SaBS: Another plausible approach is to find the real Jordan form of $M = PJP^{-1}$ and use the fact that $M^k = PJ^kP^{-1}$. Given J , J^k has a closed form formula in terms of entries of J . However, computing the Jordan form takes $\mathcal{O}(n^3)$ time, and then after this one would still need to compute $M^t \mathbf{x}_0$ for each t which is $\mathcal{O}(n^2 T)$, which provides an overall worse time complexity. Note that we cannot use the prior result [36] since in this plausible approach we do not use the same matrix in multiple matrix-vector products.

How do u_i, v_i, w_j only depend on $\mathbf{c}, \mathbf{x}, P$? Recall $M = PJP^{-1}$ where J is the real Jordan form of M and P is a real invertible matrix. The expression $\langle \mathbf{c}, M^t \mathbf{x} \rangle = \mathbf{c}^\top P J^t P^{-1} \mathbf{x}$. Consider $\sigma := P^\top \mathbf{c}$, $\tau := P^{-1} \mathbf{x}$. Then

$$\begin{aligned}
\langle \mathbf{c}, M^t \mathbf{x} \rangle &= \boldsymbol{\sigma}^\top J^t \boldsymbol{\tau} = \begin{bmatrix} \sigma_1 \\ \vdots \\ \sigma_{2q} \\ \sigma_{2q+1} \\ \vdots \\ \sigma_{2q+p} \end{bmatrix}^\top \begin{bmatrix} r_1^t J_1^t & & & & & \\ & \ddots & & & & \\ & & r_q^t J_q^t & 0 & & \\ & & & \lambda_1^t & & \\ 0 & & & & \ddots & \\ & & & & & \lambda_p^t \end{bmatrix} \begin{bmatrix} \tau_1 \\ \vdots \\ \tau_{2q} \\ \tau_{2q+1} \\ \vdots \\ \tau_{2q+p} \end{bmatrix} = \\
&\sum_{i=1}^q r_i^t \begin{bmatrix} \sigma_{2i-1} \\ \sigma_{2i} \end{bmatrix}^\top J_i^t \begin{bmatrix} \tau_{2i-1} \\ \tau_{2i} \end{bmatrix} + \sum_{j=1}^p \lambda_j^t \sigma_{2q+j} \tau_{2q+j}. \text{ Each summand in the first summation looks} \\
&\text{like } r_i^t \begin{bmatrix} \sigma_{2i-1} \\ \sigma_{2i} \end{bmatrix}^\top J_i^t \begin{bmatrix} \tau_{2i-1} \\ \tau_{2i} \end{bmatrix} = r_i^t (\cos t\theta_i(\tau_{2i-1}\sigma_{2i-1} + \tau_{2i}\sigma_{2i}) - \sin t\theta_i(\tau_{2i}\sigma_{2i-1} - \tau_{2i-1}\sigma_{2i})). \\
&\text{Defining } u_i := \tau_{2i-1}\sigma_{2i-1} + \tau_{2i}\sigma_{2i}, v_i := \tau_{2i}\sigma_{2i-1} - \tau_{2i-1}\sigma_{2i}, w_j := \tau_{2q+j}\sigma_{2q+j} \text{ for each } 1 \leq i \leq q, 1 \leq j \leq p \text{ gives } \langle \mathbf{c}, M^t \mathbf{x} \rangle = \sum_{i=1}^q r_i^t (u_i \cos t\theta_i - v_i \sin t\theta_i) + \sum_{j=1}^p w_j \lambda_j^t. \text{ Moreover, the } u_i, v_i, w_j \text{'s are defined in terms of } \boldsymbol{\sigma}, \boldsymbol{\tau} \text{ which only depend on } P, \mathbf{c}, \boldsymbol{\tau} \text{ which all have only real entries.}
\end{aligned}$$

D Additional Experiments

D.1 Computational Advantage of Converting Markov chain to GAS

By reducing the matrix M to \bar{M} , we reduce its size from $n \times n$ to $(n-1) \times (n-1)$ while keeping all the essential information intact. Asymptotically, this is of the same order but practically, it has consequences in compute times. To show a practical advantage of using \bar{M} instead of M , we ran the following experiment. Set parameters $k = 5000, n = 75, T = 10^{10}$. We generate a matrix M of size $n \times n$ randomly k times, reduce it to $\bar{M} = AMB$ (with a smaller size as in Section 3 of our paper); then compute the matrix powers M^T and \bar{M}^T . We look at each individual run and record what percentage of those k runs has a lower running time for \bar{M} and also look at their respective total running times. Let the total times (for k runs) be t_1, t_2 for M, \bar{M} respectively. We repeat this entire experiment 5 times independently and then report these percentages and the percentage decrease from t_1 to reach t_2 , namely $x = \frac{t_1 - t_2}{t_1} * 100$. In other words, computation of \bar{M}^T takes $x\%$ less time than the computation of M^T . All percentages are rounded to the nearest integer. This is shown in the table below.

Experiment run	% won	% reduction in time
1	79	25
2	77	31
3	75	44
4	75	31
5	77	37

D.2 A Use Case

We show a simple simulated experiment to illustrate how our approach could be used. We choose a 5×5 matrix with $q = 2, p = 1$ as in Eq. 1, with randomly chosen $\theta_1, \theta_2, r_1, r_2, \lambda$. We choose $\mathcal{T} = \{10, \dots, 40\}$ with a true distribution \mathbf{p} being the binomial distribution over

\mathcal{T} . In our experiment, $\mathbf{x}_0 = \begin{bmatrix} 1 \\ 2 \\ -1 \\ 0 \\ 4 \end{bmatrix}, \mathbf{c} = \begin{bmatrix} 1 \\ 2 \\ 5 \\ -2 \\ 1 \end{bmatrix}$ and M was chosen to be of the form

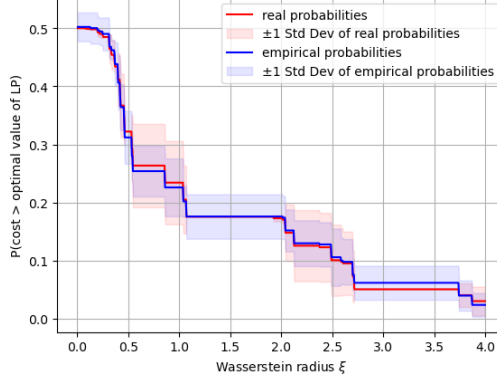


Figure 3: Real vs empirical probabilities mean (line) and standard deviation (shaded) over the five iterations.

$$\begin{bmatrix} r_1 \cos \theta_1 & r_1 \sin \theta_1 \\ -r_1 \sin \theta_1 & r_1 \cos \theta_1 \\ & \ddots \\ r_2 \cos \theta_2 & r_2 \sin \theta_2 \\ -r_2 \sin \theta_2 & r_2 \cos \theta_2 \\ & \lambda \end{bmatrix}$$
 was randomly generated parameters. The resulting M was $\begin{bmatrix} -0.973329 & 0.099035 \\ -0.099035 & -0.973329 \\ & 0.050908 & -0.019521 \\ & 0.019521 & 0.050908 \\ & & 0.451323 \end{bmatrix}$. Note that, given any cost threshold C and \mathbf{p} , we can compute real $\mathbb{P}_{\mathbf{p}}[Cost > C]$ as $\sum_{t|\langle \mathbf{c}, M^t \mathbf{x}_0 \rangle > C} p_t$.

Then we do five runs of the following experiment. Obtain 100 samples from \mathbf{p} to construct the empirical distribution $\hat{\mathbf{p}}$. Consider $\xi \in \{0.005 \cdot i : 1 \leq i \leq 800\}$. For each such ξ , we solve the LP (Eq. 3) with this empirical $\hat{\mathbf{p}}$, and obtain the optimal cost κ_ξ . For each ξ , we then compute the real and sample probabilities $\mathbb{P}_{\mathbf{p}}[Cost > \kappa_\xi]$ and $\mathbb{P}_{\hat{\mathbf{p}}}[Cost > \kappa_\xi]$. The average with std. dev. over the five runs is shown for varying ξ in Figure 3. Given the closeness of the real and empirical probabilities, we can determine an operating point with guarantees of incurring cost less than κ_ξ with probability that can be read off from the graph.

The table below for $\mathbb{P}_{\mathbf{p}}[cost > C]$ and $\mathbb{P}_{\hat{\mathbf{p}}}[cost > C]$ where $C = \langle \mathbf{c}, M^{\lfloor \hat{\mu} \rfloor} \mathbf{x} \rangle$ with $\hat{\mu}$ being the empirical mean for each of the five runs. This shows that just using the sample mean does not give a low probability of cost exceeding C , and also showing a large variation for the different runs (that have different sets of 100 data samples).

iteration	$\hat{\mu}$	$\mathbb{P}_{\mathbf{p}}[cost > C]$	$\mathbb{P}_{\hat{\mathbf{p}}}[cost > C]$
1	25.38	0.1776	0.22
2	24.69	0.6146	0.69
3	24.75	0.6146	0.59
4	25.17	0.1776	0.2
5	24.6	0.6146	0.59